Electrical Power and Energy Systems 157 (2024) 109793

Contents lists available at ScienceDirect

International Journal of Electrical Power and Energy Systems

journal homepage: www.elsevier.com/locate/ijepes

A new iterative mixed integer linear programming based real time energy efficient management of AC-DC distribution networks

Subho Paul [a,b,*], Narayana Prasad Padhy [c,d]

[a] School of Electrical Engineering and Computer Science, Washington State University, Pullman, WA, 99163, USA
[b] Department of Electrical Engineering, Indian Institute of Technology (BHU) Varanasi, Uttar Pradesh 221005, India
[c] Department of Electrical Engineering, Indian Institute of Technology Roorkee, Roorkee, Uttarakhand, 247667, India
[d] Director, Malaviya National Institute of Technology Jaipur, Jaipur, Rajasthan, 302017, India

ARTICLE INFO

Keywords:
AC-DC distribution network
Conservation voltage reduction
Iterative mixed integer linear programming
Load curtailment
Real time energy management

ABSTRACT

In the smart grid era, AC-DC distribution networks are evolving for integrating massive amounts of distributed energy resources, especially battery associated solar power generation units, into distribution networks in most energy efficient ways. Performing real time energy management for such networks is challenging due to presence of different power electronic converters, grid-edge devices and voltage controlling equipment. Existing studies either focused on developing offline day ahead methods, or shortsighted greedy strategies by neglecting the offline beneficial attributes in real time optimization frameworks. On the contrary, this article proposes a novel real time AC-DC distribution network energy management portfolio by merging load control and conservation voltage reduction techniques to achieve energy efficient operation of the network by regulating the operation of the controllable resources. Initially, the overall optimization problem is developed as a mixed integer non-convex programming by modelling the offline benefits as time coupled stochastic expressions in real time optimization platform. The non-convex expressions are later simplified by adopting different linearization techniques and the entire energy management framework is revised as a simple mixed integer linear programming (MILP). The original problem is decoupled for each time step by simplifying the time coupled expressions using virtual queues and Lyapunov functions. Additionally, a new iterative MILP algorithm is proposed to solve the revised energy management problem with less computation complexity and time. Unlike the previous solution methods, the proposed algorithm initializes the variables by their median values and handles the infeasibilities by adding tangential cutting plane constraints and penalty variable minimization objective. Demonstrating on 33-bus AC-DC distribution network, the superiority of the proposed real time energy management process and iterative MILP algorithm is established after comparing with standard energy management portfolios and existing solution methods.

1. Introduction

1.1. Motivation and prior arts

The conflict between alternating current (AC) and direct current (DC) systems came to an end in 19th century when AC systems outperformed DC systems because of its multiple benefits [1]. Due to this, the entire electricity sector is reformed as an AC system by inventing fossil fuel-based AC generators, AC transmission and distribution network architectures, and different AC loads. However, since last few decades a boost in power requirement due to urbanization and industrial revolutions is experienced [2]. Over exploitation of the fossil fuels for meeting this excess but unavoidable energy demand is causing serious environmental threat. Under this condition, green energy resources especially solar PV based DC power generation is coming up as a boon to the modern power grids. In order to reduce power conversion losses, DC network is again paving its way with the utilization of battery associated

* Corresponding author at: Department of Electrical Engineering, Indian Institute of Technology (BHU) Varanasi, Uttar Pradesh 221005, India
E-mail addresses: subho.paul@wsu.edu, subho.eee@itbhu.ac.in (S. Paul), nppadhy@ee.iitr.ac.in (N. Prasad Padhy).

https://doi.org/10.1016/j.ijepes.2024.109793
Received 30 June 2023; Received in revised form 12 November 2023; Accepted 9 January 2024
Available online 17 January 2024

Nomenclature

Abbreviations, Sets and Indices

AC/DC	Alternating current/Direct current
MILP	Mixed integer linear programming
PV	Photovoltaic
OPF	Optimal power flow
VSC	Voltage source converter
MINCP	Mixed integer non-convex programming
MICP	Mixed integer convex programming
SOCP	Second order conic programming
CVR	Conservation voltage reduction
VVC	Volt-VAR controlling
LC	Load curtailment
OA	Outer approximation
K	Set of customer types, indexed by 'k'
Γ	Set of total time steps, indexed by 't'
N_{AC}, N_{DC}	Set of AC and DC buses, indexed by 'i' and 'j'
Δt	Gap between two consecutive time steps
G, J	Set of downstream and upstream buses connected with the node 'i'

Parameters

$p_{k,i,t}^{l,\min/max}$	Minimum/maximum active power demand of customer type 'k' at bus 'i' at time 't' in kW
PF_i	Power factor at AC bus 'i'
β_i	Service quality boundary value at bus 'i'
Z_k^p, I_k^p, P_k^p	ZIP coefficient for active power demand of customer type 'k'
Z_k^q, I_k^q, P_k^q	ZIP coefficient for reactive power demand of customer type 'k'
$V_{AC}^{n/\min/\max}$	Nominal/minimum/maximum bus voltage magnitude of AC buses in kV
$V_{DC}^{n/\min/\max}$	Nominal/minimum/maximum bus voltage magnitude of DC buses in kV
$p_{i,t}^{pv}$	Active power generation from PV panel placed at bus 'i' at time 't' in kW
s_i^{pv}, s_i^b	PV and battery inverter rating placed at bus 'i' at time 't' in kVA
$e_i^{b\min/\max}$	Minimum/maximum energy limits for the battery placed at bus 'i' in kWh
$p_i^{b\max}$	Power rating of the battery placed at bus 'i' in kW
$q_{i,r}^{cb}$	Rating of capacitor bank placed at bus 'i' in kVAR
ξ_i^{vr}, ξ_i^{cb}	Maximum allowable tap operations and switching over the total time period for voltage regular and capacitor banks placed at bus 'i', respectively
r_{ij}^{ac}, x_{ij}^{ac}	Resistance and reactance of AC lines in ohm
s_{ij}^f	Distribution line thermal limit in kVA
r_{ij}^{dc}	Resistance of DC lines in ohm
α_{vsc}, η_{vsc}	VSC loss coefficient and efficiency
s_i^{vsc}	VSC rating in kVA
ς_t	Real time energy price in $/kWh
χ_t	Time dependent parameter to convert load curtailment into equivalent monetary cost in $/kWh
γ_k	Priority factor set for customer type 'k'

Decision Variables

$p_{k,i,t}^l$ and $q_{k,i,t}^l$	Actual active and reactive power demand of customer type 'k' at bus 'i' at time 't' in kW and kVAR, respectively
$p_{k,i,t}^{lcvr}$ and $q_{k,i,t}^{lcvr}$	Voltage dependent Actual active and reactive power demand of customer type 'k' at bus 'i' at time 't' in kW and kVAR, respectively
$V_{i,t}$	Bus voltage magnitude at bus 'i' at time 't' in kV
$q_{i,t}^{pv}$	Reactive power dispatch from inverter associated with PV panel placed at bus 'i' at time 't' in kVAR
$p_{i,t}^b$	Active power dispatch from inverter associated with battery placed at bus 'i' at time 't' in kW
$q_{i,t}^b$	Reactive power dispatch from inverter associated with battery placed at bus 'i' at time 't' in kVAR
$e_{i,t}^b$	Battery energy level at time 't' in kWh
$H_{i,t}^{vr}$	Tap position in the voltage regulator, placed at bus 'i' at time 't'
$q_{i,t}^{cb}$	Reactive power dispatch from the capacitor bank placed at bus 'i' at time 't' in kVAR
$A_{i,t}^{cb}$	Switching status of capacitor bank placed at bus 'i' at time 't', 0-OFF, 1-ON
$p_{i,t}^{ac,vsc}$ and $q_{i,t}^{ac,vsc}$	Active and reactive power at AC side of the VSC in kW and kVAR, respectively
$p_{ij,t}^{f,ac}, q_{ij,t}^{f,ac}$	Active and reactive power flow between two AC buses at time 't' in kW and kVAR, respectively
$I_{ij,t}^{ac}, I_{ij,t}^{dc}$	Current flowing between two AC (or two DC) buses at time 't' in kAmp
$p_{i,t}^{dc,vsc}$	Active power at DC side of the VSC in kW
$p_{ij,t}^{f,dc}$	Active power flow between two DC buses at time 't' in kW
$V_{i,t}^{ac/dc,vsc}$	AC/DC side voltage magnitude of VSC in kV
$m_{i,t}$	Modulation index of VSC at time 't'
$p_{i,t}^{l,vsc}$	Active power loss in VSC at time 't' in kW
p_t^{stn}, q_t^{stn}	Active and reactive power purchase at the main substation in kW and kVAR, respectively

PV panels, recently evolved DC power electronics loads (like LED lights, electric vehicles etc.) and smart power electronics converters. Unification of these new DC networks along with the conventional AC system framed the new AC-DC hybrid power network architectures.

Traditionally, high voltage DC links were integrated with the transmission networks for long distance power transmission [3]- [8]. Cao et al. [3] proposed a security constrained OPF topology considering N-1 contingency. Pizano-Martinez et al. [4] developed a new HVDC voltage source converter (VSC) model that the AC-DC transmission network could be solved using conventional Newton-Raphson algorithm. Rabiee and Soroudi [5] proposed a non-convex OPF strategy for an AC transmission network having uncertain wind power generation connected through a HVDC link. Venzke and Chatzivasileiadis [6] propounded a semidefinite relaxed convex optimal power flow algorithm by considering wind power generation uncertainty. Li et al. [7] proposed a multi-objective energy management process for obtaining both economic and environmental benefits. A bi-level solution approach where particle swarm optimization was implemented to obtain a Pareto optimal solution at initial level followed by the fuzzy c-means method to select the best optimal decision, was developed. González-Cabrera et al. [8] suggested a linear OPF formulation by introducing a new shift factor for AC-DC system with VSCs. Piecewise linearization was utilized to convert the non-linear terms to their equivalent linear counterparts. Sarhan at al. [9] proposed a teaching–learning-based optimization (TLBO) method for optimizing the operation of an high voltage AC network with DC links considering technical, economic and environmental constraints.

Penetration of DC distributed energy resources (PV panels and batteries) and DC loads into the distribution grids necessitate the deployment of AC-DC hybrid distribution networks with VSCs. Initially the AC-DC system is realized as the lumped microgrid in the distribution system. In this context, reference [10] performed day ahead energy cost risk minimized energy management in a residential AC-DC microgrid considering solar power and energy price uncertainties as Beta probability distribution and interval + polyhedral uncertainty, respectively. Zhao et al. [11] proposed a MILP framework for regulating the operations of the AC and DC loads in a residential microgrid to achieve minimum electricity bill. Kim et al. [12] developed a two-stage p-robust framework for energy management in an AC-DC microgrid considering uncertain power generation from solar and wind sources, load demand and energy price. A hybrid demand response portfolio by merging price and incentive based demand response is incorporated in the optimization framework and the entire problem is solved by Gaussian based regularized particle swarm optimization (PSO) with a fuzzy clustering technique. Another stochastic two-stage energy management process for AC-DC microgrid is designed by Li et al. in [13]. The two stage framework is proposed by considering the uncertain load and renewable energy generation while ensuring the frequency security in the system. Initially the relation between maximum frequency deviation and the amount of available power reserve is determined. This maximum frequency deviation constraint is used in day ahead and intraday scheduling stages for determining the optimal decisions. Cimen et al. [14] developed a bi-level online energy management strategy where at first a deep learning based non-intrusive load monitoring algorithm is used to separate the cumulative energy demand signal into individual device level and then feed to the local and global optimization frameworks for determining the load and generation schedules respectively. Kim et al. [15] proposed an Artificial Neural Network (ANN) based energy management strategy for AC-DC microgrid to determine the operation mode and charging/discharging schedule of the batteries. The proposed ANN model is a twostep process where operating mode is decided in the former one and then that input is considered at the later one to obtain the battery schedule. Another AC-DC microgrid energy management method by combining ANN and multi-objective PSO (MOPSO) is developed in [16]. The proposed AC-DC microgrid architecture for commercial buildings can reconfigure itself depending upon the system load condition and ANN is used to model the stochastic behaviour of the load and renewable generation. The MOPSO is utilized to minimize the energy cost and maximize the reliability simultaneously.

The above literatures [10–16] limited their study for lumped AC-DC microgrid and neglected the distribution network architecture. Hence, the problems are comparatively easy due to omission of complex non-convex power flow constraints. Investigations on obtaining power flow solutions for AC-DC distribution networks were carried out by utilizing Newton-Raphson [17], unified [18,19], backward-forward sweep [20], and graph theory [21,22] based algorithms without performing any economic analysis. Genetic algorithm (GA) based optimal planning strategy was developed in [23,24], and [25] considering converter life time, critical loads, and network resource capacities, respectively. Gao et al. [26] and Zhang et al. [27] planned optimal configuration of AC-DC distribution network employing non-dominated sorting genetic algorithm (NSGA-II).

In order to investigate the energy management process, Ahmed and Salama [28] designed a MILP based deterministic offline day ahead AC-DC distribution network energy management considering network reconfiguration. A deterministic volt-VAR optimization (VVO) was proposed in [29] accounting constant power critical loads by improving the node voltage quality using volt-VAR controlling (VVC) devices. The optimal solutions were obtained by employing evolutionary algorithm. Another constant power load model based VVO was designed in [30] as a mixed integer quadratic problem, where the power management was performed as a Stackelberg game between the network operator and individual microgrid operators. Luo et al. [31] aimed to minimize the loss in a multi-voltage level AC-DC distribution network by leveraging the coordinated operation of stationary storages, electric vehicles and deferrable loads. The overall problem was formulated as a MILP by linearizing the non-linear power flow constraints. A multi-objective VVO was developed in [32] by integrating a novel loss model of power electronics transformer with the forward–backward sweep power flow algorithm for AC-DC distribution networks. NSGA-II was used to solve the reactive power optimization strategy to minimize power loss and voltage deviation. A non-convex AC-DC network reconfiguration portfolio using AC and DC soft open points (SOPs) was suggested by Khan et al. [33] to minimize the network power loss. Zhu et al. [34] also proposed a multi-objective optimal scheduling method having AC and DC SOPs for reducing renewable energy curtailment and energy cost. The overall problem was framed as a MINCP and solved by hybrid GA-interior point method (GA-IPM). Alshammari et al. [35] proposed a semidefinite programming relaxed OPF algorithm for AC-DC distribution networks having different power electronics converters. A spatial and temporal scheduling of electric vehicle charging/discharging operations was investigated by Luo et al. [36]. The entire optimization method was formulated as a MILP and the optimal solutions are determined by using GUROBI solver.

To account the real time uncertainties into the offline day ahead energy management, Eajal et al. [37] proposed a bi-level stochastic method by modelling uncertain solar power generation, load demand and energy price as normal probability distribution. The overall problem was formulated as MINCP. Another bi-level stochastic optimization method based on Stackelberg game was propounded in [38]. The non-convex power flow model was relaxed using SOCP and the overall problem was designed as min–max-min robust mixed integer convex programming (MICP) to consider the effect of renewable power generation uncertainty. Gao et al. [39] employed ∞-norm and 1-norm based data-driven methodology to include wind power generation uncertainty in AC-DC distribution network management. Initially, an alternating direction method of multipliers (ADMM) based distributed OPF algorithm was proposed followed by a polyhedral linearization based linear programming solution methodology. Xu et al. [40] also developed an ADMM based robust optimization framework by modelling the load and renewable generation uncertainties as zero mean uncertainty where their variations are known in prior. A GA based stochastic energy management framework is suggested in [41] after modelling intermittent wind power generation as normal probability distribution. To leverage the benefit of load flexibility in day ahead price-based demand response, Zhao et al. [42] designed a SOCP relaxed AC-DC distribution network management process. The uncertainty involved with load flexibility was realized with fuzzy membership function and included into the dispatch model. Sun et al. [43] proposed a SOCP relaxed MICP for active and reactive power dispatch schedule in a AC-DC network. Considering droop control schemes of the VSC, the robust optimization framework was developed by considering a finite uncertainty set for the renewable power generation. Dong et al. [44] investigated the risk of high penetration of electric vehicles into the AC-DC network. Modelling the uncertainties related to the wind power, solar power, load demand and electric vehicle charging period as Weibull, Beta, Normal and Normal probability distributions, the stochastic optimization strategy was solved as a MILP. Previously, authors also proposed a risk constrained energy management strategy for AC-DC network in [45] by merging day ahead load shifting with conservation of voltage reduction (CVR). Initially the problem was developed as MINCP and later solved

with successive MILP (s-MILP) strategy by linearizing the non-linear expressions. Gholami et al. [46] also proposed a risk constrained energy management process by modelling the uncertain load, renewable power generation and EV power requirement using information-gap decision theory. The optimal decisions regarding EV management in AC-DC distribution system is determined by solving the overall problem using MILP solver.

Literatures [28–45] mainly aim to design day ahead optimization models for AC-DC distribution networks. Therefore, at real time those optimal decisions cannot be altered as per the online situation. In order to develop real time optimization strategies, Wu et al. [47] proposed a Markov decision process based real time method to reconfigure AC-DC network during extreme events like main grid outage etc. However, this deep reinforcement learning based method needs knowledge regarding the previous states and environment conditions for updating the states according to real time scenario. Shaaban et al. [48] proposed an online electric vehicle charging method to maximize the satisfaction level of electric vehicles' owners. The overall problem was developed as MINCP and solved with the non-convex commercial solver present in GAMS. Azzouz et al. [49] proposed a real time voltage regulation process by controlling the operation of electric vehicle, distributed generation and on-load tap changer. The overall method was separated into three stages to maximize the energy delivery to the electric vehicles, maximize the extracted power from distributed generation and minimize the voltage deviation consecutively. The MINCP optimization frameworks were solved by the commercial solver present in GAMS. Su et al. [50] designed a hierarchical distributed AC-DC distribution network management system by leveraging the cloud-edge collaboration. In the proposed three-layer control strategy, top layer performs day ahead analysis, middle layer does intra-day analysis and real time control is done in bottom layer. The overall problem is formulated as SOCP relaxed convex programming and solved using branch and bound method. However, multi-layer cloud based control make the approach complex for real time application.

1.2. Existing research limitations

It is worthy to mention by looking at the above literature survey that for last few years, the researches on AC-DC distribution network have gained much interest. Both day-ahead offline and real time algorithms are developed for obtaining optimal decisions. However, the existing strategies suffer from following limitations,

1. Most of the energy management topologies are developed as day ahead offline analyses [28–45] because those considers the long-term advantages like overall energy cost minimization and VVC device operation with safe limit, over the entire time period. However, the deterministic methods [28–36] require errorless forecasted input data, as they neglect real time uncertainties, and the stochastic methods [37–45] need proper probabilistic modelling of the uncertain parameters. Therefore, any inaccurate estimation of the future events makes those analyses improper for real time application.
2. Very few studies have been conducted on the real time energy management of AC-DC networks. The existing methods [47–49] do not require any knowledge of future events and consider the present values of the input data by neglecting any time coupled offline advantageous attributes. Therefore, they are mostly developed as short-sighted greedy process, i.e., the impacts of current optimal decisions on the long-term operation of network facilities and energy cost are left uncared.
3. The existing methods considered only critical loads and have not adopted any load reduction strategy for efficient management of the networks. Though, reference [29] deployed VVO but still modelled the loads as constant power type i.e., CVR is abandoned. Previously author tried to merge load shifting and CVR on day ahead optimization platform in [45]. However, integration of load control and

Table 1
Comparison table between the proposed and existing methods.

References	Year	AC-DC microgrid	AC-DC network resources			Load model		Time of analysis		Required data type				Offline beneficial aspects	Load management	Conservation voltage reduction (CVR)	Solution method
			Renewable	Battery	VVC	Constant power	Voltage dependent	Offline	Real time	Deterministic	Stochastic	Historical	Present				
[10]	2019	✓				✓		✓			✓			✓	✓		MILP
[11]	2015	✓				✓		✓		✓				✓	✓		MILP
[12]	2021	✓				✓		✓			✓			✓	✓		Gaussian based PSO
[13]	2023	✓				✓		✓			✓			✓	✓		MILP
[14]	2022	✓				✓			✓			✓	✓		✓		Deep learning and MILP
[15]	2023	✓				✓			✓			✓					ANN
[16]	2022	✓				✓		✓				✓		✓	✓		ANN- MOPSO
[28]	2019		✓			✓		✓		✓				✓			MILP
[29]	2020		✓	✓	✓	✓		✓		✓				✓			Evolutionary algorithm
[31]	2023		✓	✓		✓		✓		✓				✓	✓		MILP
[37]	2016		✓	✓		✓		✓			✓			✓			MINCP
[38]	2020		✓	✓		✓		✓			✓			✓			MICP
[45]	2021		✓	✓	✓		✓	✓			✓			✓	✓	✓	s-MILP
[46]	2022		✓	✓		✓		✓			✓			✓	✓		MILP
[47]	2022		✓	✓		✓			✓			✓	✓				Reinforcement learning
[48,49]	2015		✓	✓		✓			✓				✓				MINCP
[50]	2023		✓			✓		✓	✓	✓				✓	✓		MICP
This article	2023		✓	✓	✓		✓		✓				✓	✓	✓	✓	Iterative MILP

CVR is still left unexplored for real time optimization of AC-DC distribution network to obtain energy efficient operation. Solving such problems in real time is very challenging due to presence of highly non-convex power flow model of AC-DC network, several integer and continuous decision variables in a single optimization framework.

4. The energy management frameworks are developed as MINCP. Due to lack of good solution techniques for MINCP, different commercial MINCP solvers are used in [37,48], and [49]. However, those are expensive and are not accessible to wide number of researchers. References [29] and [34] employed different heuristic search solution algorithms but those suffers from convergence issues and may stick to local optimum solutions. SOCP relaxed MICP based power flow model is adopted in [38,42], and [43]. The MICP problems are generally solved by different decomposition methods (like benders' decomposition, outer approximation etc.) [51]. Decomposition methods confirm global optimality but take longer time to converge. Thus, not suitable for solving real time optimization frameworks. Fast converging MILP formulations are developed in [8,28] and [39] by using piecewise and polyhedral linearization methods. However, optimal solutions derived from such MILP methods influenced by the total number of linear segments considered for the non-linearity. More number of linear segments produce higher accurate results in expense of more solution time. In [45] authors proposed a new successive MILP (s-MILP) algorithm to solve the MINCP based AC-DC energy management problem by iteratively solving a relaxed MILP OPF problem. However, the prior technique requires to solve a non-convex problem for initialization to avoid OPF infeasibilities. That increases the solution time and computation complexity significantly.

1.3. Research contributions and organizations

In view with the above-mentioned research limitations, this article elucidates a novel energy efficient management portfolio for AC-DC distribution networks by merging load management (i.e., load curtailment) with CVR in real time optimization platform. Unlike the offline deterministic strategies, the proposed research framework does not need any forecasted data regarding solar power generation, load demand and energy price, and also does not need their probability distribution function to estimate their actual variation at real time (like the stochastic offline methods). On the contrary the proposed method works on the real time data and able to determine the optimal decisions. In addition to that, unlike the existing greedy real time frameworks which do not considers the long term benefits, it also considers the offline advantageous attributes as time coupled stochastic expressions in the optimization problem and used a new iterative MILP algorithm is proposed to determine the optimal decisions. The taxonomy Table 1 describes the difference between the existing and the present researches.

Initially, the proposed real time optimization framework is developed as a MINCP problem by modelling the operational constraints of the network resources (like PV panels, batteries, loads, and volt-VAR controlling devices), active and reactive power flow in the AC lines, DC lines and the VSCs. The modelling work considers the long term beneficial constraints of the network resources as time coupled stochastic expressions. Now, for easy implementation of the proposed method, all non-linear expressions are approximated by their equivalent linear counterparts and the time coupled expressions are simplified by utilizing virtual queues and Lyapunov functions. After adopting the above mentioned simplifications, the original real time MINCP problem is realized as a simple real time MILP problem. The optimal decisions are determined by solving the MILP problem iteratively. The new iterative MILP algorithm does not require initialization by solving the non-convex problem to avoid infeasibility. Instead of that, the proposed algorithm takes median start process initialization and iteratively solves a simple MILP problem by adding tangential cutting planes to avoid infeasibilities in the following iterations. The original contributions are summarized below:

1. *Problem formulation:* A new real time energy management framework for AC-DC distribution network is proposed by including offline long-term advantages as time coupled stochastic expressions into the optimization problem. To avoid difficulties of dealing with such expressions during solution process, combination of virtual queues and Lyapunov optimization is utilized to obtain a simple time decoupled MINCP framework to solve at every time interval separately.
2. *Solution technique:* The non-linear terms in the original MINCP formulation are removed by equivalent linear expressions by employing auxiliary variables and first order Taylor series approximations. Unlike the previously developed successive MILP strategy suggested in [45], the newly proposed iterative MILP process does not need to solve the integer constraint relaxed original non-convex problem to find the initial point of the Taylor series expansions. On the contrary, this algorithm takes median process initialization. Again, to avoid infeasibilities, tangential cutting plane constraints and minimization of penalty due to infeasibilities are included in the revised MILP problem. This enforces the infeasible solutions obtained at prior iteration to come back to the feasible region in the subsequent iterations.
3. *Case study demonstration and comparative analyses:* Demonstrating on modified 33 bus AC-DC test system, it is shown that the proposed energy efficient real time energy management process can successfully accommodate offline beneficial aspects while determining optimal decisions in lesser solution time. The new proposed iterative MILP process converges nearer to the global optimal point and generate AC-DC OPF feasible decisions using simple MILP commercial solvers. Further, comparative analyses show that the proposed iterative MILP algorithm outperforms existing decomposition based MICP, piecewise linearization-based MILP, and s-MILP [45] solution processes as far as the solution time and optimality gaps are concerned.

The remaining article is organized as follows: Section 2 describes the proposed real time AC-DC hybrid distribution network management problem by narrating the analytical models of all the network resources. Proposed solution process i.e., virtual queues, Lyapunov functions and iterative MILP are elaborated in section 3. Section 4 narrates two standard energy management methods used for comparing with the proposed framework. Section 5 deals with the detailed case study demonstration on 33 bus AC-DC distribution network followed by the comparative analyses with existing state of the art techniques. Finally, section 6 concludes the entire article.

2. Real time AC-DC distribution network management problem

This section describes the real time energy management portfolio of AC-DC hybrid distribution networks. The network contains smart inverter associated distributed energy resources (PV panels and batteries), voltage regulators and capacitor banks as VVC devices, VSCs for AC-DC power conversion and vice-versa, and different types of consumers (like residential, commercial) at the nodes. Initially the real time models of the network resources are discussed followed by the description on the objective function of the energy management process.

2.1. Voltage dependent load modeling

Acquiring data regarding real time operating status of individual appliance of an entire distribution system at the central controller of the main substation for load management is a strenuous job and results huge communication burden. So, in this article real time load management (i.e., load curtailment abbreviated as LC) is performed on the total active power demand of each type of consumers present at a node. Generally, real time LC is adopted prior to the application of CVR [52]. So, in the load model, the optimal load demand of any type of consumer after performing LC at each node is modelled as the voltage dependent demand. LC process targets to keep the actual load demand within the boundary limits as expressed below,

$$p_{k,i,t}^{l,\min} \leqslant p_{k,i,t}^{l} \leqslant p_{k,i,t}^{l,max} \tag{1}$$

Therefore, total power demand at node 'i' is given below,

$$p_{i,t}^{l} = \sum_{k\in K} p_{k,i,t}^{l}, p_{i,t}^{l,\min} = \sum_{k\in K} p_{k,i,t}^{l,\min}, p_{i,t}^{l,max} = \sum_{k\in K} p_{k,i,t}^{l,max} \tag{2}$$

The consumer wise and total reactive power demand at the AC buses can be expressed as follows,

$$q_{k,i,t}^{l} = p_{k,i,t}^{l}\sqrt{\left(1/PF_i^2\right) - 1}, q_{i,t}^{l} = \sum_{k\in K} q_{k,i,t}^{l} \tag{3}$$

Now, frequent load curtailment at a particular bus may cause large discomfort to the consumers present at that bus. Therefore, to restrict the load curtailment process, following constraint is added in offline studies [45].

$$\frac{1}{\Gamma}\sum_{t\in\Gamma}\left[\frac{p_{i,t}^{l,max} - p_{i,t}^{l}}{p_{i,t}^{l,max} - p_{i,t}^{l,\min}}\right] \leqslant \beta_i \tag{4}$$

Constraint (4) signifies that the total average load curtailment for a particular bus must be lower than the service quality boundary value (β_i) for that particular node. Constraint (4) forces the energy management process to refrain from large amount of demand curtailment and that restores the service quality. However, incorporation of constraint (4) requires the knowledge about the total time period 'Γ' and the future load demands. However, in real time this information is not available and highly uncertain. Therefore, the constraint (4) is revised as a stochastic expression as written below,

$$\lim_{\Gamma\to\infty}\frac{1}{\Gamma}\sum_{t=0}^{\Gamma-1}\mathrm{E}\left[\frac{p_{i,t}^{l,max} - p_{i,t}^{l}}{p_{i,t}^{l,max} - p_{i,t}^{l,\min}}\right] \leqslant \beta_i \tag{5}$$

where, E[.] represents the expected value calculation operator. Constraint (5) tries to keep the expected value of the uncertain average load curtailment for the infinite time period below the service quality boundary. Therefore, indirectly this constraint restricts the LC operation at each time step in real time.

Now as per [52], the CVR topology will be implemented after determining the optimal demand of any consumer at a particular node. Therefore, after adopting ZIP load model the consumers' active and reactive power demands are as follows,

$$p_{k,i,t}^{lcvr} = p_{k,i,t}^{l}\left(Z_k^p u_{i,t} + I_k^p v_{i,t} + P_k^p\right) \tag{6}$$

$$\left.\begin{aligned} q_{k,i,t}^{lcvr} &= q_{k,i,t}^{l}\left(Z_k^q u_{i,t} + I_k^q v_{i,t} + P_k^q\right) \\ \Rightarrow q_{k,i,t}^{lcvr} &= p_{k,i,t}^{l}\left(\sqrt{\left(1/PF_i^2\right) - 1}\right)\left(Z_k^q u_{i,t} + I_k^q v_{i,t} + P_k^q\right) \end{aligned}\right\} \tag{7}$$

here, $Z_k, I_k,$ and P_k are the ZIP load coefficients for active and reactive power demand of consumer type 'k', such that $Z_k + I_k + P_k = 1$ and

$$\left(\frac{V_i^{\min}}{V_i^n}\right) \leqslant v_{i,t} \leqslant \left(\frac{V_i^{\max}}{V_i^n}\right), \text{ and } \left(\frac{V_i^{\min}}{V_i^n}\right)^2 \leqslant u_{i,t} \leqslant \left(\frac{V_i^{\max}}{V_i^n}\right)^2 \tag{8}$$

$$\text{here, } v_{i,t} = \left(\frac{V_{i,t}}{V_i^n}\right), u_{i,t} = \left(\frac{V_{i,t}}{V_i^n}\right)^2, V_i^{n/\min/\max} = \begin{cases} V_{AC}^{n/\min/\max}, i \in N_{AC} \\ V_{DC}^{n/\min/\max}, i \in N_{DC} \end{cases}$$

2.2. Modeling of distributed energy resources

As mentioned before, in this article PV panels and batteries are accounted as distributed energy resources. These energy resources are associated with smart inverters to regulate the active and reactive power dispatches. The operating constraints of these distributed energy resources are given below.

$$0 \leqslant q_{i,t}^{pv} \leqslant \sqrt{\left(s_i^{pv}\right)^2 - \left(p_{i,t}^{pv}\right)^2} \tag{9}$$

$$e_{i,t}^{b} = e_{i,t-1}^{b} + p_{i,t}^{b}\Delta t \tag{10}$$

$$e_i^{b\min} \leqslant e_{i,t}^{b} \leqslant e_i^{b\max} \text{ and } -p_i^{b\max} \leqslant p_{i,t}^{b} \leqslant p_i^{b\max} \tag{11}$$

$$\left(p_{i,t}^{b}\right)^2 + \left(q_{i,t}^{b}\right)^2 \leqslant \left(s_i^{b}\right)^2 \tag{12}$$

Inequality (9) represents the boundary limit of the reactive power dispatch from solar inverters. The battery energy level updating process at each time is done by the equality constraint (10) (assuming 100 % battery efficiency). The battery energy level and the active power dispatch from the battery inverters are limited by the inequalities presented in (11). The reactive power dispatch from the battery inverter is related with the inverter capacity and the active power dispatch by the inequality constraint (12).

2.3. Modeling of Volt-VAR controlling (VVC) devices

Generally, the CVR operation tends to lower the bus voltage magnitude. However, to keep the voltage magnitude within the safety limit, VVC devices like voltage regulators and capacitor banks are employed. The operating constraints of those VVC devices are mentioned below.

$$V_{j,t} = V_{i,t} + 0.00625 \times H_{i,t}^{vr} \times V_i^n, \forall i \in N_{AC} \tag{13}$$

$$-16 \leqslant H_{i,t}^{vr} \leqslant 16 \tag{14}$$

$$q_{i,t}^{cb} = A_{i,t}^{cb} q_{i,r}^{cb} w_{i,t}, w_{i,t} = \left(V_{i,t}\right)^2 \tag{15}$$

The voltage of the downstream bus 'j' is modified with the help of voltage regulator placed at bus 'i' by following equation (13). The regulator has total 32 tap positions, where 16 tap positions are used to lower the voltage magnitude and other 16 are used for voltage magnitude increasing. This tap position limits are given in (14). The reactive power dispatch from the capacitor banks are given by equation (15).

Now, tap changers and capacitor bank switches are mechanical devices. So, the life of voltage regulators and capacitor banks are highly impacted by multiple tap changing and switching operations respectively [53]. Therefore, to restrict the frequent operation in voltage regulators and the capacitor banks, constraints (16) and (17) are added in the offline studies [53].

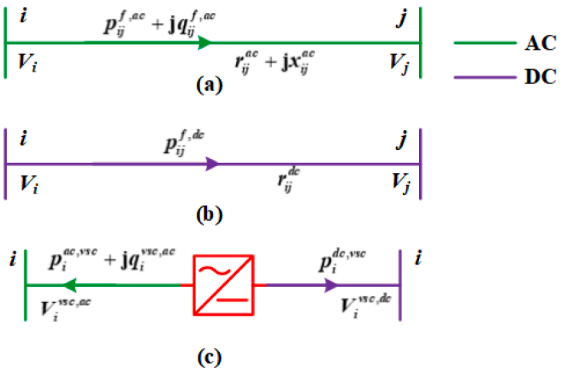

Fig. 1. AC-DC distribution network architectures, (a) AC to AC connection, (b) DC to DC connection, and (c) voltage source converter (VSC) station.

$$\sum_{t\in\Gamma}\left|H_{i,t}^{vr} - H_{i,t-1}^{vr}\right| \leqslant \xi_i^{vr} \tag{16}$$

$$\sum_{t\in\Gamma}\left|A_{i,t}^{cb} - A_{i,t-1}^{cb}\right| \leqslant \xi_i^{cb} \tag{17}$$

Constraints (16) and (17) denote that the total number of tap changing and switching operations over the entire time period 'Γ' must be below the maximum allowable boundary limits. Now, constraints (16) and (17) are offline constraints, so they cannot be directly incorporated to real time optimization framework due to reasons mentioned in section 2.1. Hence, these constraints are converted to their real time counterparts by writing them as a time average stochastic equalities as follows,

$$\lim_{\Gamma\to\infty}\frac{1}{\Gamma}\sum_{t=0}^{\Gamma-1}\mathrm{E}\left[\left|H_{i,t}^{vr} - H_{i,t-1}^{vr}\right|\right] \leqslant \xi_i^{vr} \tag{18}$$

$$\lim_{\Gamma\to\infty}\frac{1}{\Gamma}\sum_{t=0}^{\Gamma-1}\mathrm{E}\left[\left|A_{i,t}^{cb} - A_{i,t-1}^{cb}\right|\right] \leqslant \xi_i^{cb} \tag{19}$$

2.4. Power flow model of AC-DC distribution network

The AC-DC hybrid distribution networks mainly consists of AC buses, DC buses and VSCs for AC to DC conversion and vice versa. Depending upon these components, the overall network can be segregated into three sectors as shown in Fig. 1. Three sectors are AC network, DC network and VSC station. The power flow constraints corresponding those sectors are written below [45].

$$p_{i,t}^{ac,net} = \left(\sum_{k\in K} p_{k,i,t}^{lcvr}\right) - p_{i,t}^{pv} - p_{i,t}^{b} - p_{i,t}^{ac,vsc} \tag{20}$$

$$q_{i,t}^{ac,net} = \left(\sum_{k\in K} q_{k,i,t}^{lcvr}\right) - q_{i,t}^{pv} - q_{i,t}^{b} - q_{i,t}^{cb} - q_{i,t}^{ac,vsc} \tag{21}$$

$$p_{i,t}^{ac,net} + \sum_{g\in G} p_{ig,t}^{f,ac} = \sum_{j\in J}\left(p_{ji,t}^{f,ac} - r_{ij}^{ac} I_{ji,t}^{ac}\right), \forall t, i \in N_{ac} \tag{22}$$

$$q_{i,t}^{ac,net} + \sum_{g\in G} q_{ig,t}^{f,ac} = \sum_{j\in J}\left(q_{ji,t}^{f,ac} - x_{ij}^{ac} I_{ji,t}^{ac}\right), \forall t, i \in N_{ac} \tag{23}$$

$$w_{j,t} = w_{i,t} - 2\left[r_{ij}^{ac} p_{ij,t}^{f,ac} + x_{ij}^{ac} q_{ij,t}^{f,ac}\right] + \left(\left(r_{ij}^{ac}\right)^2 + \left(x_{ij}^{ac}\right)^2\right) I_{ij,t}^{ac}, \forall (i,j) \in N_{ac} \tag{24}$$

$$w_{i,t} I_{ij,t}^{ac} = \left(p_{ij,t}^{f,ac}\right)^2 + \left(q_{ij,t}^{f,ac}\right)^2, I_{ij,t}^{ac} = \left(I_{ij,t}^{ac}\right)^2, \forall (i,j) \in N_{ac} \tag{25}$$

$$\left(p_{ij,t}^{f,ac}\right)^2 + \left(q_{ij,t}^{f,ac}\right)^2 \leqslant \left(s_{ij}^{f}\right)^2, \forall (i,j) \in N_{ac} \tag{26}$$

$$p_{i,t}^{dc,net} = \left(\sum_{k\in K} p_{k,i,t}^{lcvr}\right) - p_{i,t}^{pv} - p_{i,t}^{b} - p_{i,t}^{dc,vsc} \tag{27}$$

$$p_{i,t}^{dc,net} + \sum_{g\in G} p_{ig,t}^{f,dc} = \sum_{j\in J}\left(p_{ij,t}^{f,dc} - r_{ij}^{dc} I_{ij,t}^{dc}\right), \forall t, i \in N_{dc} \tag{28}$$

$$w_{j,t} = w_{i,t} - 2\left[r_{ij}^{dc} p_{ij,t}^{f,dc}\right] + \left(r_{ij}^{dc}\right)^2 I_{ij,t}^{dc}, \forall (i,j) \in N_{dc} \tag{29}$$

$$w_{i,t} I_{ij,t}^{dc} = \left(p_{ij,t}^{f,dc}\right)^2, I_{ij,t}^{dc} = \left(I_{ij,t}^{dc}\right)^2, \forall (i,j) \in N_{dc} \tag{30}$$

$$p_{ij,t}^{f,dc} \leqslant s_{ij}^{f}, \forall (i,j) \in N_{dc} \tag{31}$$

$$V_{i,t}^{ac,vsc} = 0.612 m_{i,t} V_{i,t}^{dc,vsc} \tag{32}$$

$$p_{i,t}^{ac,vsc} + p_{i,t}^{dc,vsc} + p_{i,t}^{l,vsc} = 0 \tag{33}$$

$$\left(p_{i,t}^{ac,vsc}\right)^2 + \left(q_{i,t}^{ac,vsc}\right)^2 = \left(p_{i,t}^{l,vsc}/\alpha_{vsc}\right)^2 \tag{34}$$

$$p_{i,t}^{ac,vsc} = (1/\eta_{vsc}) p_{i,t}^{dc,vsc} \tag{35}$$

$$\left(p_{i,t}^{ac,vsc}\right)^2 + \left(q_{i,t}^{ac,vsc}\right)^2 \leqslant \left(s_i^{vsc}\right)^2 \tag{36}$$

$$\left(V_i^{\min}\right)^2 \leqslant w_{i,t} \leqslant \left(V_i^{\max}\right)^2, w_{i,t} = \left(V_{i,t}\right)^2, \forall i \in [N_{ac}, N_{dc}] \tag{37}$$

$$p_t^{stn} = \sum_{i\in N_{ac}} p_{i,t}^{ac,net} + \sum_{i\in N_{dc}} p_{i,t}^{dc,net} + \sum_{i\in N_{ac}}\sum_{j\in N_{ac}} r_{ij}^{ac} I_{ij,t}^{ac} + \sum_{i\in N_{dc}}\sum_{j\in N_{dc}} r_{ij}^{dc} I_{ij,t}^{dc} + \sum_{i\in[N_{ac},N_{dc}]} p_{i,t}^{l,vsc} \tag{38}$$

$$q_t^{stn} = \sum_{i\in N_{ac}} q_{i,t}^{ac,net} + \sum_{i\in N_{ac}}\sum_{j\in N_{ac}} x_{ij}^{ac} I_{ij,t}^{ac} \tag{39}$$

In the above power flow expressions, (20) -(26) are associated with the AC network. Net active and reactive power requirement at any AC bus are given in (20) and (21) respectively. Active and reactive power balance are done at AC buses by following equations (22) and (23) respectively. The voltage at any AC bus and current flowing between two AC buses are represented in (24) and (25) respectively. AC line flow capability is restricted by inequality (26). Similarly, expressions (27) -(31) represent the DC network. The net active power demand and the active power balance at DC buses are given by (27) and (28) respectively. Bus voltage, line current and power flow expressions are depicted in (29), (30) and (31) respectively. The VSC stations are modelled by expressions (32) -(36). The AC and DC side voltages are interrelated by equation (32) [54]. Active power balance and active power loss at VSC are expressed in (33) and (34) respectively. Constraint (35) relates the DC side active power with the AC side active power and vice versa. The total apparent power transaction through VSC follows constraint (36). Bus voltage magnitudes of AC and DC buses are restricted by their corresponding boundary limits, as shown in (37). The active and reactive power transactions at the substation node follows power balance equations (38) and (39) respectively.

2.5. Energy management objective function

The real time energy management process aims to determine the

optimal control decisions for the above-mentioned network resources at every time interval by minimizing the below mentioned objective function.

$$C_t = \varsigma_t\left(p_t^{stn}\cdot\Delta t\right) + \chi_t \sum_{i\in[N_{AC},N_{DC}]}\sum_{k\in K}\left(\gamma_k\cdot\left(p_{i,t}^{l,max} - p_{i,t}^{l}\right)\Delta t\right), \chi_t \geqslant 0, \forall t \in \Gamma \quad (40)$$

Objective function (40) consists of two separate terms. Former term represents the total monetary energy cost paid by the network operator to the upper grid operator. Last term signifies the total dissatisfaction experienced by each consumer type present at any bus location due to load curtailment in terms of monetary loss. This dissatisfaction cost is included by the network operator into the objective function to maintain the service quality. It is noted from the dissatisfaction cost that dissatisfaction is zero for a particular type of consumer if its maximum amount of requested demand is met, else it will take positive values.

Conventionally, CVR or Volt-VAR optimization considers distribution network loss minimization as objective function [53,55]. However, in case of CVR, voltage reduction causes more network loss [55] and that inherently increases the power purchase from the upper grid through the main substation. Therefore, minimization of monetary energy cost will try to minimize the network loss during CVR implementation.

Now, it is evident from different offline researches like day-ahead energy management [28–45] and network planning [26,27], that the operation of the network resources can be controlled at most optimal way (like discharging of battery power at peak load hours and charging at off-peak load hours) if the optimization algorithm considers long term or the summed value of the objective function for the entire time period as minimizing quantity. However, as total number of time period and the future situations are unknown in real time optimization, so the long-term value of the objective function (40) can be written as stochastic expression (41) by considering infinite number of time period and expected value of the C_t.

$$\lim_{\Gamma\to\infty}\sum_{t\in\Gamma}\mathrm{E}[C_t] \quad (41)$$

Therefore, at each time step the objective function is the time average value of (41) and the overall energy management portfolio is as follows.

$$\mathrm{Min}\lim_{\Gamma\to\infty}\left(\frac{1}{\Gamma}\sum_{t\in\Gamma}\mathrm{E}[C_t]\right) \quad (42)$$

Subject to, (1) -(3), (5) -(15), and (18) -(39).

3. Solution process

It can be seen that the above-described energy management framework possesses non-convexity and also has time coupled stochastic expressions as objective function and constraints. Direct solution of such optimization problem is not possible at every time step separately, and needs to adopt some simplification strategies. This section illustrates some simplification techniques to convert the previously described complex energy management portfolio into a simple MILP. In addition, an iterative algorithm is designed to obtain the optimal decisions.

3.1. Linearization technique

The linearization techniques are adopted to replace the non-convex expressions like absolute functions (|.|), bilinear and quadratic terms by their equivalent linear equivalents. The simplification processes are described below.

3.1.1. Auxiliary variables for absolute functions

Auxiliary variables are used to omit the non-convex expressions related to absolute functions and bilinear terms. Constraints (18) and (19) have absolute functions. These absolute functions can be easily linearized by the positive auxiliary variables $h_{i,t}^{vr} = \left|H_{i,t}^{vr} - H_{i,t-1}^{vr}\right|$ and $a_{i,t}^{cb} = \left|A_{i,t}^{cb} - A_{i,t-1}^{cb}\right|$. Therefore, the revised constraints are as follows,

$$\lim_{\Gamma\to\infty}\frac{1}{\Gamma}\sum_{t=0}^{\Gamma-1}\mathrm{E}\left[h_{i,t}^{vr}\right] \leqslant \xi_i^{vr} \quad (43)$$

$$\lim_{\Gamma\to\infty}\frac{1}{\Gamma}\sum_{t=0}^{\Gamma-1}\mathrm{E}\left[a_{i,t}^{cb}\right] \leqslant \xi_i^{cb} \quad (44)$$

Such that,

$$h_{i,t}^{vr} \geqslant H_{i,t}^{vr} - H_{i,t-1}^{vr} \text{ and } h_{i,t}^{vr} \geqslant H_{i,t-1}^{vr} - H_{i,t}^{vr} \quad (45)$$

$$a_{i,t}^{cb} \geqslant A_{i,t}^{cb} - A_{i,t-1}^{cb} \text{ and } a_{i,t}^{cb} \geqslant A_{i,t-1}^{cb} - A_{i,t}^{cb} \quad (46)$$

Capacitive reactive power supply equation (15) consists of product of two variables where $u_{i,t}$ is continuous variable and $A_{i,t}^{cb}$ is binary. Now, considering the boundary values of $u_{i,t}$ and defining an auxiliary variable $f_{i,t}^{cb} = A_{i,t}^{cb} w_{i,t}$, the equation (15) is rewritten as,

$$q_{i,t}^{cb} = q_{i,n}^{cb} f_{i,t}^{cb} \quad (47)$$

Such that,

$$w_{i,t} - \left(V_i^{\max}\right)^2\left(1 - A_{i,t}^{cb}\right) \leqslant f_{i,t}^{cb} \leqslant w_{i,t} - \left(V_i^{\min}\right)^2\left(1 - A_{i,t}^{cb}\right) \quad (48)$$

$$\left(V_i^{\min}\right)^2 A_{i,t}^{cb} \leqslant f_{i,t}^{cb} \leqslant \left(V_i^{\max}\right)^2 A_{i,t}^{cb} \quad (49)$$

It is noted, when $A_{i,t}^{cb} = 1$, constraint (48) makes $f_{i,t}^{cb} = w_{i,t}$. Again, when $A_{i,t}^{cb} = 0$, constraint (49) makes $f_{i,t}^{cb} = 0$.

3.1.2. McCormick envelopes for bilinear terms

McCormick envelopes are generally utilized to realize the bilinear terms (which is a product of two continuous variables) [56]. The bilinear terms are present at the active and reactive power demand models (6) and (7), and the VSC voltage conversion equation (32). According to [56], any bilinear term 'ab', (having boundaries $a \in [a_L, a_U]$, $b \in [b_L, b_U]$), can be represented as the auxiliary variable $d = ab$, subject to the McCormick envelope constraints written below,

$$\left.\begin{array}{l} d \geqslant ab_U + a_U b - a_U b_U, d \geqslant ab_L + a_L b - a_L b_L \\ d \leqslant ab_U + a_L b - a_L b_U, d \leqslant ab_L + a_U b - a_U b_L \end{array}\right\} \quad (50)$$

These envelope approximations are called to be tight or accurate if at the optimal decision the optimal values d^*, a^* and b^* satisfies the original multiplicity i.e., $d^* = a^* b^*$. However, Shukla et al. [57] proved the inexactness of the McCormick envelopes for long range continuous variables (i.e., gap between upper and lower bounds of variable is large). Therefore, for successful implementation of McCormick envelopes, both variables should have small gaps between their corresponding upper and lower bounds. Now, from expressions (6), (7) and (32), that the envelopes need to be formed for the terms $p_{k,i,t}^{l} u_{i,t}$, $p_{k,i,t}^{l} v_{i,t}$, and $m_{i,t} V_{i,t}^{dc,vsc}$. Now, $v_{i,t}$ and $u_{i,t}$ in (6) and (7) denote per-unit and square of per-unit values of the phase voltages respectively. Therefore, range of these per-unit variables are obviously very low (safe limit of phase voltages are 1.05 pu to 0.95 pu, hence range of $v_{i,t}$ and $u_{i,t}$ are 0.05 and 0.0025 respectively). However, range of active power demand variable $p_{k,i,t}^{l}$ is

very large during the LC operation (normally in terms of MW). Forming envelopes with the actual values of the active power demand variables may suffer from exactness issues and can cause large optimality gap. Therefore, in order to restore exactness in the approximation process, the envelopes are applied on the per unit load models with the auxiliary variables, $d_{1,k,i,t} = \left(p^{l}_{k,i,t}/s_b\right)u_{i,t}$ and $d_{2,k,i,t} = \left(p^{l}_{k,i,t}/s_b\right)v_{i,t}$. Therefore, the revised load models are written as (51) and (52), subject to the equivalent constraint (50) corresponding to each auxiliary variable.

$$\frac{p^{lcvr}_{k,i,t}}{s_b} = Z^{p}_{k} d_{1,k,i,t} + I^{p}_{k} d_{2,k,i,t} + P^{p}_{k}\frac{p^{l}_{k,i,t}}{s_b} \tag{51}$$

$$\frac{q^{lcvr}_{k,i,t}}{s_b} = \left(\sqrt{\left(1/PF^{2}_{i}\right)-1}\right)\left(Z^{q}_{k} d_{1,k,i,t} + I^{q}_{k} d_{2,k,i,t} + P^{q}_{k}\frac{p^{l}_{k,i,t}}{s_b}\right) \tag{52}$$

Again, in (32) both variables $m_{i,t}$ cannot be varied in a large range as the modulation index of any inverter is mostly set close to unity. However, DC bus voltages range in a large range of several kV. Therefore, for tightness the per unit DC bus voltage value is considered and an auxiliary variable $d_{3,i,t} = m_{i,t}\left(V^{dc,vsc}_{i,t}/V^{n}_{DC}\right)$ is proposed and included in the optimization framework the envelopes (50) corresponding to it. Hence, the linearized VSC voltage equation is as written in (53).

$$V^{ac,vsc}_{i,t} = 0.612 d_{3,i,t} V^{n}_{DC} \tag{53}$$

3.1.3. First order Taylor series for quadratic constraints

Presence of quadratic equality constraints in the AC-DC distribution network power flow model also add non-convexity to the energy management problem. Authors of [38] and [30] implemented SOCP relaxations to obtain the global optimality. However, solution time for a SOCP relaxed mixed integer convex optimization framework is quite large and not suitable for real time energy management process. So, here each quadratic term in the constraints (12), (25), (26), (30), (34) and (36) are expanded by using first order Taylor series. The linear constraints at the evaluation point at iteration 'x' are written below (the solution points are depicted by putting a hat (^) on the variable),

$$2p^{b}_{i,t}\left(\widehat{p}^{b}_{i,t}\right)^{x} + 2q^{b}_{i,t}\left(\widehat{q}^{b}_{i,t}\right)^{x} - \left[\left(\widehat{p}^{b}_{i,t}\right)^{x}\right]^{2} - \left[\left(\widehat{q}^{b}_{i,t}\right)^{x}\right]^{2} \leqslant \left(s^{b}_{i,t}\right)^{2} \tag{54}$$

$$l^{ac}_{ij,t}\left(\widehat{w}_{i,t}\right)^{x} + w_{i,t}\left(\widehat{l}^{ac}_{ij,t}\right)^{x} = 2p^{f,ac}_{ij,t}\left(\widehat{p}^{f,ac}_{ij,t}\right)^{x} + 2q^{f,ac}_{ij,t}\left(\widehat{q}^{f,ac}_{ij,t}\right)^{x} - \left[\left(\widehat{p}^{f,ac}_{ij,t}\right)^{x}\right]^{2} - \left[\left(\widehat{q}^{f,ac}_{ij,t}\right)^{x}\right]^{2} \tag{55}$$

$$2p^{f,ac}_{ij,t}\left(\widehat{p}^{f,ac}_{ij,t}\right)^{x} + 2q^{f,ac}_{ij,t}\left(\widehat{q}^{f,ac}_{ij,t}\right)^{x} - \left[\left(\widehat{p}^{f,ac}_{ij,t}\right)^{x}\right]^{2} - \left[\left(\widehat{q}^{f,ac}_{ij,t}\right)^{x}\right]^{2} \leqslant \left(s^{f}_{ij}\right)^{2} \tag{56}$$

$$l^{dc}_{ij,t}\left(\widehat{w}_{i,t}\right)^{x} + w_{i,t}\left(\widehat{l}^{dc}_{ij,t}\right)^{x} = 2p^{f,dc}_{ij,t}\left(\widehat{p}^{f,dc}_{ij,t}\right)^{x} - \left[\left(\widehat{p}^{f,dc}_{ij,t}\right)^{x}\right]^{2} \tag{57}$$

$$2p^{ac,vsc}_{i,t}\left(\widehat{p}^{ac,vsc}_{i,t}\right)^{x} + 2q^{ac,vsc}_{i,t}\left(\widehat{q}^{ac,vsc}_{i,t}\right)^{x} - \left[\left(\widehat{p}^{ac,vsc}_{i,t}\right)^{x}\right]^{2} - \left[\left(\widehat{q}^{ac,vsc}_{i,t}\right)^{x}\right]^{2} = \left(\frac{1}{\alpha_{vsc}}\right)^{2}\left[2p^{l,vsc}_{i,t}\left(\widehat{p}^{l,vsc}_{i,t}\right)^{x} - \left[\left(\widehat{p}^{l,vsc}_{i,t}\right)^{x}\right]^{2}\right] \tag{58}$$

$$2p^{ac,vsc}_{i,t}\left(\widehat{p}^{ac,vsc}_{i,t}\right)^{x} + 2q^{ac,vsc}_{i,t}\left(\widehat{q}^{ac,vsc}_{i,t}\right)^{x} - \left[\left(\widehat{p}^{ac,vsc}_{i,t}\right)^{x}\right]^{2} - \left[\left(\widehat{q}^{ac,vsc}_{i,t}\right)^{x}\right]^{2} \leqslant \left(s^{vsc}_{i}\right)^{2} \tag{59}$$

Therefore, the final linearized real time energy efficient AC-DC hybrid distribution management portfolio is given below,

$$\left.\begin{aligned} &\text{Min } \lim_{\Gamma\to\infty}\left(\frac{1}{\Gamma}\sum_{t\in\Gamma}\mathrm{E}[C_t]\right) \\ &\text{subject to, (1) - (3), (5), (8) - (11), (13), (14), (20) - (24), (27) - (29), (31), (33), (35), (37) - (39), and (43) - (59)} \end{aligned}\right\} \tag{60}$$

3.2. Relaxation of time coupled expressions

Solving the energy management problem (60) is still complex as the objective function and the constraints (5), (43) and (44) are time coupled in nature. Further, separate time control decisions for battery charging/discharging may be optimal for the present time interval but not be good for future time steps, i.e. the battery may discharge at off-peak hours and charge at peak hours. Therefore, battery operation is also time coupled and needs the knowledge regarding future events. To relax this time coupling situations in real time optimization framework, virtual queues [58] are defined corresponding to each time coupled conditions like load curtailment, tap changing in voltage regulators, capacitor bank switching and battery charging/discharging. After defining the virtual queues, Lyapunov optimization is implemented to frame the final real time energy management portfolio to be solved at each time step.

3.2.1. Definition of virtual queues

The main purposes of the virtual queues are to restrict the load curtailment, multiple tap changing and capacitor switching, and unregulated battery operations. In this regard, four virtual queues are defined which are set at zero initially and then upgraded by following the equalities (61) -(64).

$$\mathbb{R}^{l}_{i,t+1} = \max\left(\mathbb{R}^{l}_{i,t} - \beta_i, 0\right) + \left(\frac{p^{l,max}_{i,t} - p^{l}_{i,t}}{p^{l,max}_{i,t} - p^{l,\min}_{i,t}}\right), \forall i \in [N_{AC}, N_{DC}] \tag{61}$$

$$\mathbb{R}^{vr}_{i,t+1} = \max\left(\mathbb{R}^{vr}_{i,t} - \xi^{vr}_{i}, 0\right) + h^{vr}_{i,t} \tag{62}$$

$$\mathbb{R}^{cb}_{i,t+1} = \max\left(\mathbb{R}^{cb}_{i,t} - \xi^{cb}_{i}, 0\right) + a^{cb}_{i,t} \tag{63}$$

$$\mathbb{R}^{b}_{i,t+1} = \mathbb{R}^{b}_{i,t} + p^{b}_{i,t}\Delta t \tag{64}$$

and $\mathbb{R}^{l}_{i,0} = \mathbb{R}^{vr}_{i,0} = \mathbb{R}^{cb}_{i,0} = \mathbb{R}^{b}_{i,0} = 0$

Queue (61) is associated with the load curtailment process and its length grows if load curtailment occurs. Similarly, queues (62) and (63)

are related with voltage regulators and capacitor banks respectively, and their length increases due to each tap changing and capacitor switching. Finally, battery queue, (64), length changes for every charging/discharging operation.

Now, to prevent undesired load curtailment, frequent tap changing and capacitor switching, and unregulated battery power transaction, the real time optimization must prevent the queue length upgradation at every time interval. Therefore, constraint (65) will be added into the energy management framework.

$$\lim_{t\to\infty}\frac{\mathrm{E}\left[\left|\mathbb{R}^{l}_{i,t}\right|\right]}{t}=\lim_{t\to\infty}\frac{\mathrm{E}\left[\left|\mathbb{R}^{vr}_{i,t}\right|\right]}{t}=\lim_{t\to\infty}\frac{\mathrm{E}\left[\left|\mathbb{R}^{cb}_{i,t}\right|\right]}{t}=\lim_{t\to\infty}\frac{\mathrm{E}\left[\left|\mathbb{R}^{b}_{i,t}\right|\right]}{t}=0 \tag{65}$$

3.2.2. Lyapunov optimization

Previous queue definitions relax the time coupling constraints and the battery operation, but the objective function still a time coupled expression and (65) is also a complex constraint having limit calculus. Solving an optimization framework consist of objective function and constraints with limit calculus is challenging. Therefore, certain simplification processes need to be adopted. Now, the objective function aims to restrict the energy cost and dissatisfaction increment, and the purpose of constraint (65) is to limit the queue length enhancement. Undesirable growth in the queue length due to violation of constraint (65), leads the solution to an unreliable state by violating the long term advantages. Therefore, to optimally control the solution process of the derived stochastic optimization framework, in this article Lyapunov optimization [58] is adopted to simplify the time average stochastic optimization framework. Lyapunov optimization is mainly utilized in control theory to ensure the stability of a system. The principle of Lyapunov optimization mainly relies on the choice of Lyapunov functions for doing positive scalar measurement of the chaotic parameters in a system [59]. In this paper, virtual queues are the chaotic parameters in the real time optimization problem. Hence, Lyapunov functions are developed for the four queues (61) -(64).

Now, generally quadratic functions are best suitable as the Lyapunov function for each chaotic parameter [60] and the overall system Lyapunov function is represented as the weighted sum of the functions corresponding to each chaos i.e., queues [59]. Therefore, at time interval 't' the Lyapunov function corresponding to the proposed virtual queues is as follows,

$$L(\mathbb{N}_t)=\frac{1}{2}\sum_{i\in[N_{AC},N_{DC}]}\left[\rho\left(\mathbb{R}^{l}_{i,t}\right)^2+\sigma\left(\mathbb{R}^{vr}_{i,t}\right)^2+\varepsilon\left(\mathbb{R}^{cb}_{i,t}\right)^2+\varphi\left(\mathbb{R}^{b}_{i,t}\right)^2\right] \tag{66}$$

Here, $\mathbb{N}_t=\left[\mathbb{R}^{l}_{i,t},\mathbb{R}^{vr}_{i,t},\mathbb{R}^{cb}_{i,t},\mathbb{R}^{b}_{i,t}\middle|\forall i\in[N_{AC},N_{DC}]\right]$,$\rho,\sigma,\varepsilon$ and φ are constant weights for treating the queues separately. In this article the weight values are set to 1 to avoid biasness towards any queue.

The optimal decisions may reach at undesirable condition if the Lyapunov function value grows largely. Therefore, stability can only be attained if this grow is reduced by minimizing the Lyapunov drift near to zero value. Now, the Lyapunov drift equation given in (67) is used to measure the expected growth of the previously defined queues at the present time interval 't'.

$$\Delta(\mathbb{N}_t)=\mathrm{E}[(L(\mathbb{N}_{t+1})-L(\mathbb{N}_t))\,|\mathbb{N}_t] \tag{67}$$

Reduction of this Lyapunov drift will inherently minimize the queue growth and that results lesser load curtailment and battery charging/discharging. As a result of this, the energy cost will rise. Therefore, the optimization must have a weighted trade-off objective between these two contradictory objectives as shown below,

$$U_t=\Delta(\mathbb{N}_t)+W\times\mathrm{E}[C_t|\mathbb{N}_t],W>0 \tag{68}$$

Here, W is used as a trade-off constant between two objectives.

Lemma 1. *Any feasible solution satisfies the following upper boundary condition,*

$$U_t\leqslant O+\sum_{i\in[N_{AC},N_{DC}]}\left(\begin{array}{c}\rho\mathbb{R}^{l}_{i,t}\mathrm{E}\left[\dfrac{p^{l,max}_{i,t}-p^{l}_{i,t}}{p^{l,max}_{i,t}-p^{l,\min}_{i,t}}-\beta_i\middle|\mathbb{N}_t\right]+\sigma\mathbb{R}^{vr}_{i,t}\mathrm{E}\left[h^{vr}_{i,t}-\xi^{vr}_{i}\middle|\mathbb{N}_t\right]\\+\varepsilon\mathbb{R}^{cb}_{i,t}\mathrm{E}\left[a^{cb}_{i,t}-\xi^{cb}_{i}\middle|\mathbb{N}_t\right]+\varphi\mathbb{R}^{b}_{i,t}\mathrm{E}\left[p^{b}_{i,t}\Delta t\middle|\mathbb{N}_t\right]\end{array}\right)+W\times\mathrm{E}[C_t|\mathbb{N}_t] \tag{69}$$

where, $O=0.5\sum_{i\in[N_{AC},N_{DC}]}\left[\rho\left(1+(\beta_i)^2\right)+\sigma\left(1+\left(\xi^{vr}_{i}\right)^2\right)+\varepsilon\left(1+\left(\xi^{cb}_{i}\right)^2\right)+\varphi\left(p^{b\max}_{i}\Delta t\right)^2\right]$

Proof: at Appendix A

Now, instead of minimizing the actual value of U_t, if we minimize this maximum value then the value of U_t will inherently be reduced. Therefore, only having the knowledge regarding present events and the queue lengths the optimal decisions are obtained by solving the following optimization framework (70) at every time interval. Optimization framework (70) can be easily solved as it is completely linear in nature and also time decoupled.

$$\boldsymbol{P1}\begin{cases}\text{Min }\Re_t=WC_t+\displaystyle\sum_{i\in[N_{AC},N_{DC}]}\left(\frac{\rho\mathbb{R}^{l}_{i,t}\left(-p^{l}_{i,t}\right)}{p^{l,max}_{i,t}-p^{l,\min}_{i,t}}+\sigma\mathbb{R}^{vr}_{i,t}h^{vr}_{i,t}+\varepsilon\mathbb{R}^{cb}_{i,t}a^{cb}_{i,t}+\varphi\mathbb{R}^{b}_{i,t}p^{b}_{i,t}\Delta t\right)\\ \text{subject to, (1) - (3), (8) - (11), (13), (14), (20) - (24), (27) - (29), (31), (33), (35), (37) - (39), (45) - (59), and (61) - (64)}\end{cases} \tag{70}$$

Remark 1. *With the defined Lyapunov function in expression (66), the optimal decisions obtained by solving the real time optimization problem (70) will always keep the AC-DC distribution network under stable operating condition.*

Proof: at Appendix B.

3.3. Infeasibility handling

In 3.1.3 sub-section, quadratic terms in the battery inverter capacity and AC-DC power flow constraints are revised with first order Taylor series by omitting the higher orders. The optimal solutions at iteration 'x' may violate battery inverter limit and possess AC-DC OPF infeasibilities if,

$$\left(s^{b}_{i,t}\right)^2<\left[\left(\widehat{p}^{b}_{i,t}\right)^x\right]^2+\left[\left(\widehat{q}^{b}_{i,t}\right)^x\right]^2 \tag{71}$$

$$\left[\left(\widehat{p}^{f,ac}_{ij,t}\right)^x\right]^2+\left[\left(\widehat{q}^{f,ac}_{ij,t}\right)^x\right]^2\neq\left(\widehat{w}_{i,t}\right)^x\left(\widehat{l}^{ac}_{ij,t}\right)^x \tag{72}$$

$$\left(s^{f}_{ij}\right)^2<\left[\left(\widehat{p}^{f,ac}_{ij,t}\right)^x\right]^2+\left[\left(\widehat{q}^{f,ac}_{ij,t}\right)^x\right]^2 \tag{73}$$

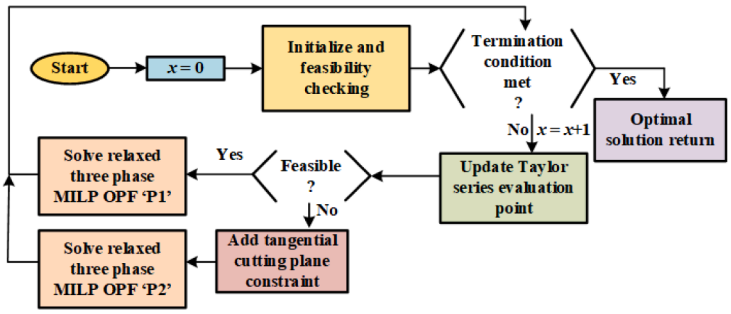

Fig. 2. Proposed iterative MILP algorithm for real time management of AC-DC distribution network.

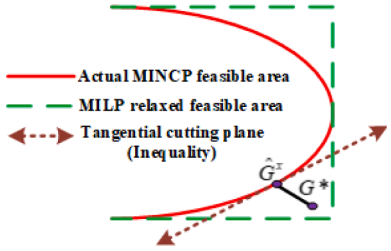

Fig. 3. Tangential cutting plane forces the infeasible solution G^* obtained at iteration 'x' to the feasible solution.

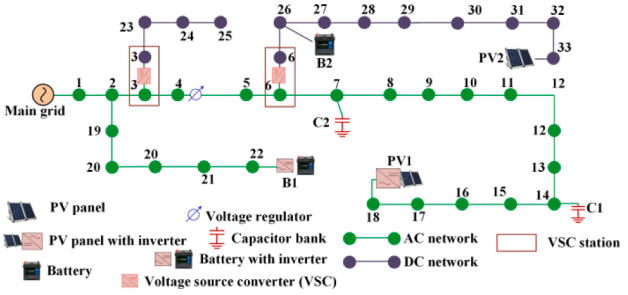

Fig. 4. Case study demonstration test system: 33-bus AC-DC distribution network.

$$\left[\left(\widehat{p}_{ij,t}^{f,dc}\right)^x\right]^2 \neq \left(\widehat{w}_{i,t}\right)^x\left(\widehat{l}_{ij,t}^{dc}\right)^x \tag{74}$$

$$\left[\left(\widehat{p}_{i,t}^{ac,vsc}\right)^x\right]^2+\left[\left(\widehat{q}_{i,t}^{ac,vsc}\right)^x\right]^2 \neq \left(\frac{1}{\alpha_{vsc}}\right)^2\left[\left(\widehat{p}_{i,t}^{l,vsc}\right)^x\right]^2 \tag{75}$$

$$\left(s_i^{vsc}\right)^2 < \left[\left(\widehat{p}_{i,t}^{ac,vsc}\right)^x\right]^2+\left[\left(\widehat{q}_{i,t}^{ac,vsc}\right)^x\right]^2 \tag{76}$$

Now, infeasibilities (72), (74) and (75) denote the following conditions,

$$\text{either } \left[\left(\widehat{p}_{ij,t}^{f,ac}\right)^x\right]^2+\left[\left(\widehat{q}_{ij,t}^{f,ac}\right)^x\right]^2 > \left(\widehat{w}_{i,t}\right)^x\left(\widehat{l}_{ij,t}^{ac}\right)^x \text{ or } < \left(\widehat{w}_{i,t}\right)^x\left(\widehat{l}_{ij,t}^{ac}\right)^x \tag{77}$$

$$\text{either } \left[\left(\widehat{p}_{ij,t}^{f,dc}\right)^x\right]^2 > \left(\widehat{w}_{i,t}\right)^x\left(\widehat{l}_{ij,t}^{dc}\right)^x \text{ or } < \left(\widehat{w}_{i,t}\right)^x\left(\widehat{l}_{ij,t}^{dc}\right)^x \tag{78}$$

$$\text{either } \left[\left(\widehat{p}_{i,t}^{ac,vsc}\right)^x\right]^2+\left[\left(\widehat{q}_{i,t}^{ac,vsc}\right)^x\right]^2 > \left(\frac{1}{\alpha_{vsc}}\right)^2\left[\left(\widehat{p}_{i,t}^{l,vsc}\right)^x\right]^2 \text{ or } < \left(\frac{1}{\alpha_{vsc}}\right)^2\left[\left(\widehat{p}_{i,t}^{l,vsc}\right)^x\right]^2 \tag{79}$$

Therefore, to bring the solutions within feasible region for the infeasibilities (71), (73) and (76), tangential cutting plane constraints (80) -(82) are added with the MILP problem.

$$p_{i,t}^{b}\left(\widehat{p}_{i,t}^{b}\right)^x+q_{i,t}^{b}\left(\widehat{q}_{i,t}^{b}\right)^x \leqslant \left(s_{i,t}^{b}\right)^2+\delta_{i,t}^{b,vio} \tag{80}$$

$$p_{ij,t}^{f,ac}\left(\widehat{p}_{ij,t}^{f,ac}\right)^x+q_{ij,t}^{f,ac}\left(\widehat{q}_{ij,t}^{f,ac}\right)^x \leqslant \left(s_{ij}^{f}\right)^2+\delta_{ij,t}^{fac,vio} \tag{81}$$

$$p_{i,t}^{ac,vsc}\left(\widehat{p}_{i,t}^{ac,vsc}\right)^x+q_{i,t}^{ac,vsc}\left(\widehat{q}_{i,t}^{ac,vsc}\right)^x \leqslant \left(s_i^{vsc}\right)^2+\delta_{i,t}^{vsc,vio} \tag{82}$$

Further, for infeasibility (77), two inequality tangential cutting planes are added with the MILP problem.

$$p_{ij,t}^{f,ac}\left(\widehat{p}_{ij,t}^{f,ac}\right)^x+q_{ij,t}^{f,ac}\left(\widehat{q}_{ij,t}^{f,ac}\right)^x \leqslant w_{i,t}\left(\widehat{l}_{ij,t}^{ac}\right)^x+\left(\widehat{w}_{i,t}\right)^x l_{ij,t}^{ac}+\chi_{ij,t}^{fac,vio+} \tag{83}$$

$$w_{i,t}\left(\widehat{l}_{ij,t}^{ac}\right)^x+\left(\widehat{w}_{i,t}\right)^x l_{ij,t}^{ac} \leqslant p_{ij,t}^{f,ac}\left(\widehat{p}_{ij,t}^{f,ac}\right)^x+q_{ij,t}^{f,ac}\left(\widehat{q}_{ij,t}^{f,ac}\right)^x+\chi_{ij,t}^{fac,vio-} \tag{84}$$

Remark: If constraints (83) and (84) are simultaneously satisfied for any solution with $\chi_{ij,t}^{fac,vio+}=\chi_{ij,t}^{fac,vio-}=0$ and the solution point does not change between iteration 'x-1' and 'x' (i.e., optimal solution point), then

$$\left[\left(\widehat{p}_{ij,t}^{f,ac}\right)^x\right]^2+\left[\left(\widehat{q}_{ij,t}^{f,ac}\right)^x\right]^2=\left(\widehat{w}_{i,t}\right)^x\left(\widehat{l}_{ij,t}^{ac}\right)^x$$

Similarly, tangential plane constraints (85), (86) are added for infeasibility (78), and (87), (88) are for infeasibility (79).

$$p_{ij,t}^{f,dc}\left(\widehat{p}_{ij,t}^{f,dc}\right)^x \leqslant w_{i,t}\left(\widehat{l}_{ij,t}^{dc}\right)^x+\left(\widehat{w}_{i,t}\right)^x l_{ij,t}^{dc}+\chi_{ij,t}^{fdc,vio+} \tag{85}$$

$$w_{i,t}\left(\widehat{l}_{ij,t}^{dc}\right)^x+\left(\widehat{w}_{i,t}\right)^x l_{ij,t}^{dc} \leqslant p_{ij,t}^{f,dc}\left(\widehat{p}_{ij,t}^{f,dc}\right)^x+\chi_{ij,t}^{fdc,vio-} \tag{86}$$

$$p_{i,t}^{ac,vsc}\left(\widehat{p}_{i,t}^{ac,vsc}\right)^x+q_{i,t}^{ac,vsc}\left(\widehat{q}_{i,t}^{ac,vsc}\right)^x \leqslant \left(\frac{1}{\alpha_{vsc}}\right)^2\left[p_{i,t}^{l,vsc}\left(\widehat{p}_{i,t}^{l,vsc}\right)^x\right]+\chi_{i,t}^{vsc,vio+} \tag{87}$$

$$\left(\frac{1}{\alpha_{vsc}}\right)^2\left[p_{i,t}^{l,vsc}\left(\widehat{p}_{i,t}^{l,vsc}\right)^x\right] \leqslant p_{i,t}^{ac,vsc}\left(\widehat{p}_{i,t}^{ac,vsc}\right)^x+q_{i,t}^{ac,vsc}\left(\widehat{q}_{i,t}^{ac,vsc}\right)^x+\chi_{i,t}^{vsc,vio-} \tag{88}$$

In constraints (80) -(88), $\delta_{i,t}^{b,vio}$, $\delta_{ij,t}^{fac,vio}$, $\delta_{i,t}^{vsc,vio}$, $\chi_{ij,t}^{fac,vio+}$, $\chi_{ij,t}^{fac,vio-}$, $\chi_{ij,t}^{fdc,vio+}$, $\chi_{ij,t}^{fdc,vio-}$, $\chi_{i,t}^{vsc,vio+}$, and $\chi_{i,t}^{vsc,vio-}$ are the penalty variables. Now, to make the solutions AC-DC OPF and inverter feasible, the penalty variable minimization is added with the objective function. Hence, the revised MILP problem is

$$\boldsymbol{P2}\begin{cases}\text{Min } \Re_t+\theta\sum_i\sum_j\left(\delta_{i,t}^{b,vio}+\delta_{ij,t}^{fac,vio}+\delta_{i,t}^{vsc,vio}+\chi_{ij,t}^{fac,vio+}+\chi_{ij,t}^{fac,vio-}+\chi_{ij,t}^{fdc,vio+}+\chi_{ij,t}^{fdc,vio-}+\chi_{i,t}^{vsc,vio+}+\chi_{i,t}^{vsc,vio-}\right)\\ \text{subject to, (1) - (3), (8) - (11), (13), (14), (20) - (24), (27) - (29), (31), (33), (35),}\\ \text{(37) - (39), (45) - (59), (61) - (64), and (80) - (88)}\end{cases} \tag{89}$$

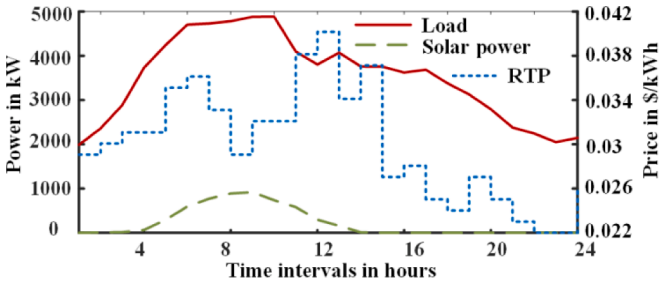

Fig. 5. Input data for case study demonstration: load, energy price, and solar power generation.

here θ is used to convert the penalty values to equivalent monetary value, and set at 0.5 in this study.

3.4. Proposed iterative mixed integer linear programming algorithm

Flow chart of the proposed iterative MILP algorithm is depicted in Fig. 2. Initially (i.e., at $x = 0$), the solution point for the first order Taylor series is approximated by the median values within their range. The AC-DC OPF feasibility of this initial point is checked by determining the power flows and if it is infeasible then it is updated to be within the feasibility region. After that the MILP problem is iteratively solved and after each iteration, the termination condition is checked, i.e., the derived solution is AC-DC OPF feasible (i.e., the values of all penalty variables are zero) and the objective function values do not change more than the tolerance limit (1e-5) for two successive iterations. If termination condition is not satisfied, then the Taylor series evaluation point is updated with the new solution point.

After revising the Taylor series point, the feasibilities are checked. If any solution point possesses either AC-DC OPF or inverter infeasibilities or both, then tangential cutting plane constraints are added with the MILP problem to enforce the feasibilities in the consecutive iterations (see Fig. 3). As noted from previous sub-section that tangential cutting plane constraints are imposed by introducing penalty variables which are minimized in the objective function. Since, the solutions are derived by solving the MILP problem having first order Taylor series approximation for replacing the non-linear terms in original MINCP problem, the convergence at global optimal point, i.e., KKT optimal solution, is guaranteed when the iterative algorithm terminates with zero values of the penalty variables.

4. Standard energy management portfolios for Comparison

Efficacy of the proposed real time energy management process is established by comparing with two standard energy management portfolios. The standard methods are described in the following sub-sections considering the objective function and constraints of this article. The standard algorithms are solved by iterative MILP algorithm after adopting certain simplification techniques described above.

4.1. Offline AC-DC energy management

Offline deterministic AC-DC energy management process is accounted as the first standard strategy, which is mainly followed in [28]- [36]. This considers the accurate future events in the analysis and works as the perfect standard tool to analyse the performance of real time studies. The offline framework is as follows,

$$\left.\begin{aligned} &\text{Min } C = \sum_{t\in T} C_t \\ &\text{subject to, (1) - (4), (6) - (17), and (20) - (39)} \end{aligned}\right\} \tag{90}$$

4.2. Real time greedy algorithm

Greedy algorithm is most well-known type of real time energy management process which does not consider offline time coupled constraints in the optimization framework [48 49]. This short-sighted strategy considers only the present event data and optimize the objective separately at every time interval. This takes the form of real time deterministic optimization portfolio as follows,

Min C_t

Subject to, (1)-(3), (6)-(15), (20)-(39) and

$$\frac{p_{i,t}^{l,max} - p_{i,t}^{l}}{p_{i,t}^{l,max} - p_{i,t}^{l,\min}} \leqslant \beta_i, \forall t, i \tag{91}$$

Table 2
Simulation results for different control cases.

Evaluated parameter	Control cases			
	Case 1: No CVR, No LC	Case 2: Yes CVR, No LC	Case 3: No CVR, Yes LC	Case 4: Yes CVR, Yes LC
Optimal peak load (kW)	4884.94	4640.48	4159.50	3945.68
Optimal minimum voltage (pu)	0.935	0.951	0.972	0.953
Optimal maximum voltage (pu)	0.987	0.976	0.992	0.991
Optimal total network loss (MW)	2.1752	2.1279	1.9624	1.8868
Total tap operations by voltage regulator	49	67	46	51
Total C1 switching	5	6	5	5
Total C2 switching	6	8	4	5

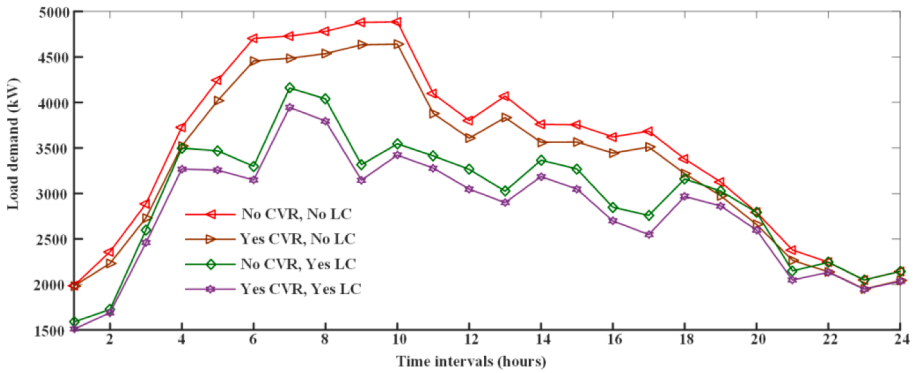

Fig. 6. Total load demand of the IEEE 33 bus test system because of different control cases.

5. Case study demonstration and comparative analyses

5.1. 33-Bus AC-DC test system

The performance of the proposed real time AC-DC distribution network management is evaluated on 33-bus AC-DC test system shown in Fig. 4 (adopted from [45]). The simulation is carried out for a day (24 h) considering 1-hour time interval. The standard IEEE 33 bus test system line data are considered while neglecting the line reactance for the DC lines. The base voltage for DC and AC sides are 20.67 kV and 12.66 kV respectively. The base MVA is set at 10 MVA. The voltage magnitude of the main sub-station (i.e., bus 1) is fixed at 1.0 pu, whereas the safe operating limits for bus voltage magnitudes are considered to be between 1.05 pu and 0.95 pu corresponding to their base values. The bus locations of the solar panels, batteries, capacitor banks and voltage regulator are shown in Fig. 4. The batteries and solar panels at the AC buses are connected through the inverters. The energy and power ratings of the batteries are 1 MWh and 0.5 MW, respectively. They can charge up to 100 % and discharge up to 30 % of its energy rating. The solar panels are of 1 MW capacity and their 24-hour power generation pattern (hourly data from 6 am of present day to 6 am of next day) is shown in Fig. 5. The hourly solar generation data is from a collection of real PV panels installed in the campus of IIT Roorkee, India. IIT Roorkee is an Indian educational institute situated at Uttarakhand district in India. The campus system has currently 1.8 MW of installed solar panel capacity. Among 1.8 MW, the solar panels of cumulative capacity 1 MW are placed in the academic section of the campus (at the rooftop of different department buildings) and its hourly generation profile is recorded and displayed at the main administrative building. In this study, authors have used the solar power generation profile on a hot summer day of June 2019 having perfect sunlight from 6:30 am to around 6 pm. The voltage regulators are allowed to perform maximum 60 tap changing in a day, and similarly the upper limit for capacitor bank switching is fixed to 6 [53]. The inverters associated with the batteries and the solar panels in AC network are of 1.5 MVA ratings. The cumulative maximum 24-hour load demand for the entire network is also shown in Fig. 5 as the red line. The load profile is also from the IIT Roorkee campus system, which experience almost 5 MW daily peak demand during summer (i.e., April to August) and around 3.5 MW of daily peak demand during winter (i.e., from November to March). The cumulative hourly load data of the entire campus is generally recorded at the main substation of the campus. The hourly load profile (6 am of present day to 6 am of next day) shown in Fig. 5 is a demand curve experienced by the IIT Roorkee campus on a hot summer day of May 2019. The critical or the minimum load demand for each hour is randomly set between 30 % and 50 % of the Fig. 5 data. The reactive power demand is calculated by considering random load factor between 0.85 and 0.95. The hourly real time energy price on 18th June 2018 is shown as dotted blue curve in Fig. 5, which is taken from [61]. The efficiency and operating power factor of VSCs are 95 % and 0.95, respectively. The values of χ_t are set at 0.025 $/kWh, 0.01 $/kWh and 0.015 $/kWh for the time intervals between 1 am and 10 am, 10 am and 8 pm, and 8 pm and 1 am, respectively. The trade-off constant 'W' is fixed at 10. The service quality limit (β_i) is 0.5 pu.

5.2. Case study simulations

The case study simulation is carried out at MATLAB 2019b, installed in a 64 bit, i7, 16 GB RAM personal computer. The MILP problem at each iteration of the proposed algorithm is solved by using 'intlinprog' commercial solver, present in MATLAB. At first, the bus loads are accounted as residential type and their ZIP coefficients are taken from [62]. The value of γ_k is set at 1.5. Four distinguished control cases are simulated to show the energy efficient operation of the 33-bus AC-DC network, viz. Case 1: No CVR, No LC, Case 2: Yes CVR, No LC, Case 3: No CVR, Yes LC, and Case 4: Yes CVR, Yes LC. When CVR is not implemented, i.e., for cases 1 and 3, the loads are considered to be of constant power type. The cumulative optimal hourly load demands for the four cases are shown in Fig. 6. The optimal values corresponding to peak load, minimum and maximum bus voltage magnitudes (in pu), total network loss, total tap changing operations of the voltage regulator and switch operations of the capacitor banks for each case are provided in Table 2.

Case 1 is simulated without considering any load reduction technique (i.e., no CVR and no LC) and by relaxing the minimum bus voltage magnitude boundary conditions. The minimum voltage boundary limits are relaxed as it is noted that during peak load hour (i.e., time interval 10), if the lower boundary limit (i.e., 0.95 pu) is imposed then to obey the power flow constraint, the optimal value of the maximum bus voltage is 1.064 pu, which denotes overvoltage condition (as the upper safe limit is 1.05 pu). Therefore, to avoid overvoltage the simulation is carried out with the upper boundary limit and relaxing the lower limit and the optimal results are shown in Table 2. It is noted that the minimum voltage value is 0.935 pu, which is quite below the safe under

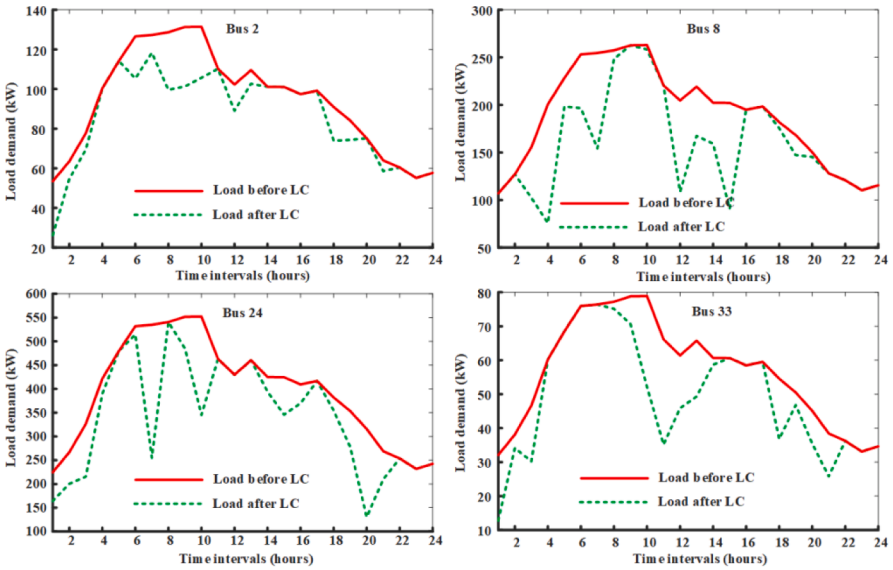

Fig. 7. Unregulated and regulated load demand at different bus positions.

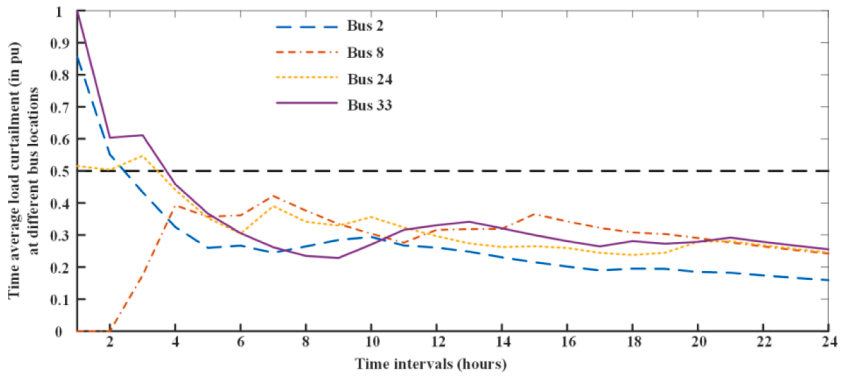

Fig. 8. Time average load curtailment (in pu) experienced by different buses.

Table 3
Peak load and total loss values for different load mix conditions.

Load mix conditions	Control cases			
	Case 1	Case 2	Case 3	Case 4
Peak load (kW)				
100 % residential	4884.94	4640.48	4159.50	3945.68
75 % residential, 25 % commercial	4884.94	4705.63	4196.86	4037.82
50 % residential, 50 % commercial	4884.94	4776.18	4269.48	4106.73
Total active power loss (MW)				
100 % residential	2.1752	2.1279	1.9624	1.8868
75 % residential, 25 % commercial	2.1752	2.1434	2.0186	1.9216
50 % residential, 50 % commercial	2.1752	2.1509	2.0753	1.9508

voltage condition (which is 0.95 pu). This indicates the requirement to adopt demand reduction techniques using CVR or LC or both.

The voltage limits are imposed for case 2 simulation, however the constraints regarding maximum tap operations of voltage regulator and switching operations of capacitor banks (i.e., constraints (18) and (19)) are relaxed. This is done, as it is observed that with the considered loading conditions and to implement CVR, the regulator needs to perform more than 60 tap operations and capacitor banks are required to do switching operations more than 6 times to maintain the voltage within the safe boundary values. Individual deployment of CVR reduces the active power demand (see brown curve in Fig. 6) by dragging down the bus voltages close to the minimum boundary value (peak demand decrement is 5.004 %). It is noted that the minimum voltage value is at 0.951 pu (Table 2). Further, the total active power loss for the network is reduced from 2.1752 MW to 2.1279 MW (hence 2.1745 % reduction). However, with the considered load curve the minimum bus voltage is kept within safety limit by performing 67 tap operations for the regulator and 8 switching operations for C2 (see Table 2). Therefore, it is worthy to adopt LC operation along with CVR, as deployment of CVR alone can reduce the load but that pushes the voltage regulator and capacitor banks to operate more than its safety limit (hence reduce their life expectancy).

Case 3 is simulated by implementing only LC considering all the operating and safety constraints. Unlike CVR, LC operation reduces the

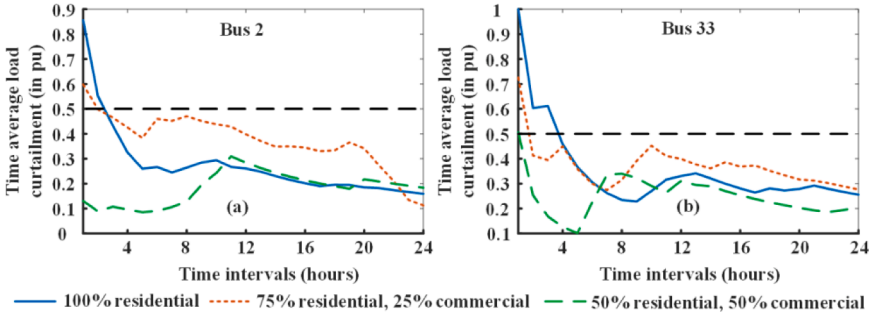

Fig. 9. Time average load curtailment (in pu) experienced due to different load mix, (a) bus 2 (AC bus), and (b) bus 33 (DC bus).

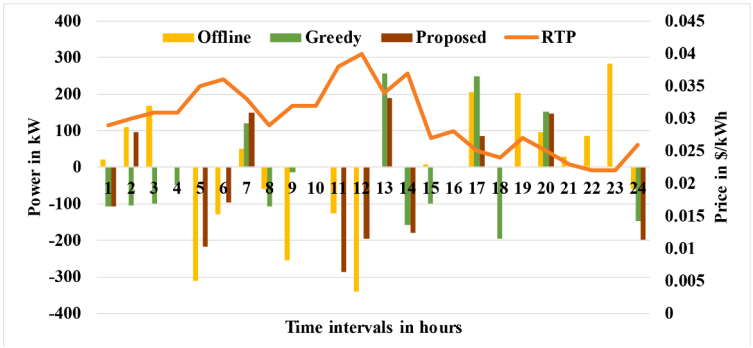

Fig. 10. Total battery power due to three different AC-DC distribution network energy management frameworks.

Table 4
Simulation outcomes for different methods.

Evaluated parameter	Methods		
	Offline	Greedy	Proposed
Optimal peak load (kW)	3710.55	4780.92	3945.68
Optimal total network loss (MW)	1.7962	2.1451	1.8868
Total energy cost ($)	1563.18	2165.29	1650.46
Total tap operations by voltage regulator	42	66	51
Total C1 switching	4	6	5
Total C2 switching	4	8	5

load demand (green curve in Fig. 6) but also improves the bus voltage magnitude (peak load is reduced by 14.8505 %). Due to that the minimum bus voltage magnitude is at 0.972 pu. Again, it is noted from Fig. 6 that the LC operation is mostly implemented during peak and mid-peak hours (hour 1 to 21). However, no LC operation is conducted during off-peak hours (i.e., hour 22 to 24) to avoid large consumer discomfort. Further, the total active power loss is reduced by 9.783 % and the VVC devices (i.e., voltage regulator and capacitor banks) are operated within their corresponding safety limits (Table 2).

It is noticed from case 2 and case 4, that both CVR and LC are helpful to reduce the peak load demand. Therefore, in case 4 these two load reductions techniques are merged and implemented on the AC-DC network. It is observed that similar to case 3 the LC operation reduces the peak and mid-peak hour demands and operates the VVC devices (i.e., regulator and capacitor banks) within their allowable maximum limits (see Table 2). The CVR implementation further reduces the active power demand and the bus voltage magnitudes are set near to the minimum boundary limit (peak reduction is 19.2277 %). The minimum bus voltage value is 0.953. In addition to the peak and mid-peak hour demand reduction, CVR reduces the consumption of the voltage dependent loads even during the off-peak hours (violet curve in Fig. 6). Due to that maximum network loss reduction (approximately 13.2586 %) is obtained in case 4. Hence, it is worthy to conclude that merger of CVR and LC (i.e., case 4) provides most energy efficient real time operation of the AC-DC distribution networks.

5.3. Fairness checking of the proposed method

Now, LC is an intrusive load reduction technique which always has tendency to curtail load demand at each time step from all the buses. However, that will create large dissatisfaction to the consumers who experience frequent load curtailment, which is not desirable. To show the fairness obtained by the proposed method, the optimized load demand at two AC buses (2 and 8) and two DC buses (24 and 33) are shown in Fig. 7. The pu time average load curtailment values of the four buses at every time step are depicted in Fig. 8. It is observed from Fig. 7, that the LC operation is implemented in distributed manner to all the buses and a certain bus is not experiencing load shedding at every time step (for both AC and DC networks). Therefore, their time average load curtailment values generally remain below the quality-of-service limit (see Fig. 8). This shows the effectiveness of the proposed method which reduces bus demand but also takes care of the customer satisfaction.

5.4. Performance analysis with different load mix conditions

To check the performance of the proposed strategy for other type of consumers, further simulation is carried out with different load mix conditions by varying the percentage of residential and commercial consumers in the total load demand at each bus at every time step. The simulation results are summarized in Table 3 for all the four cases described in previous sub-section. The ZIP load coefficients for the commercial consumers are taken from [62] and as commercial customers are less flexible for their consumption so γ_k is set at 2.5. It is observed from Table 3 that due to lesser dependence on voltage magnitude for commercial loads, the peak load and loss reduction are less if the percentage share of commercial customer is more. The time average load curtailment curves for AC bus 2 and DC bus 33 are shown in Fig. 9 for different load mix conditions. For all the conditions, the time average load curtailment values initially are high but reduce and remain under the quality service limit with rolling time intervals. However, if the commercial load share is high then to avoid large discomfort, the commercial load curtailment is low. Hence, the load curtailment pu values drop below the limit rapidly.

5.5. Comparison with standard energy management portfolios

In this section, comparative analyses are carried out between the proposed and the standard AC-DC distribution network energy management methods, described in section 4 (considering the loads are of only residential type). The comparisons are done in terms of charging/discharging of batteries, optimal values of the total energy cost and network loss, maximum voltage regulator tap operations and capacitor banks switching, time average load curtailment (pu), and cumulative energy cost at each time step. The simulation results are shown in Fig. 10, Table 4, Fig. 11 and Fig. 12.

The offline method can accommodate the long-term benefits most

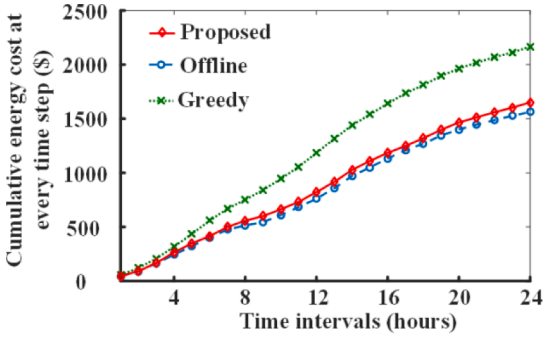

Fig 12. Cumulative energy cost at every time step for different methods.

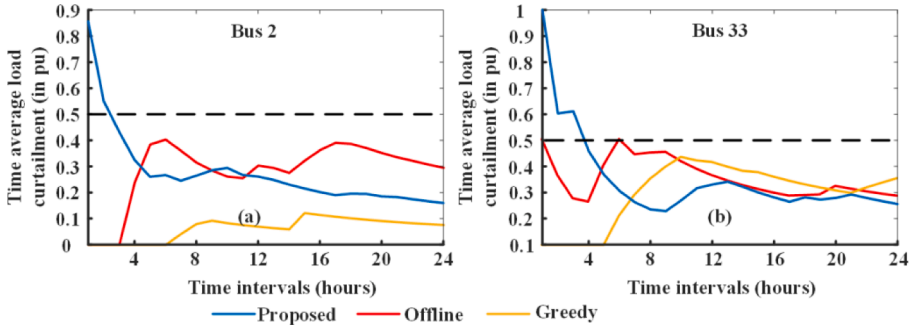

Fig. 11. Time average load curtailment (in pu) experienced due to different methods, (a) bus 2 (AC bus), and (b) bus 33 (DC bus).

Table 5
Comparative analyses between different solution methods.

Method	Number of linear segments	Total optimal energy cost ($)	Error (%)	Average number of iterations per time step	Average solution time per time step (min)
Convex relaxation (OA)	–	1648.19	– (Base case)	15	20.75
Piecewise linearization	2	1719.73	4.3045 %	–	1.24
	5	1683.46	2.1399 %	–	3.52
	10	1663.57	0.9331 %	–	5.17
	15	1650.02	0.1110 %	–	7.83
	20	1649.94	0.1062 %	–	11.29
s-MILP [45]	–	1653.87	0.3446 %	7	9.3
Proposed iterative MILP	–	1650.46	0.1377 %	4	3.67

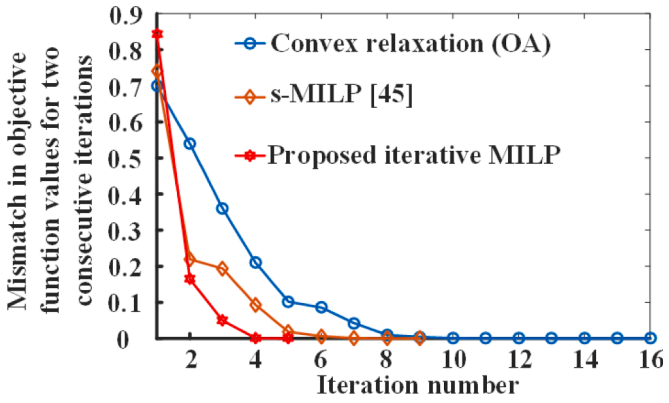

Fig. 13. Convergence curves of different solution methods at maximum loading hour (i.e., hour 10).

efficiently. It is noted that the batteries are charged at off-peak price hours, and discharged during peak and mid-peak price hours (see Fig. 10). This results lowest total energy cost and network active power loss. Again, the total voltage regulator tap operations and capacitor banks switching are below the safe boundary limits (see Table 4). The time average load curtailment for both AC and DC buses are below the service limit (see Fig. 11) and also the cumulative energy cost at each time interval is lowest (see Fig. 12). Though offline method requires accurate knowledge regarding the future events, which is difficult to obtain, but the simulation results from offline method can certainly serve as the reference to check the efficacy of the existing greedy and proposed real time AC-DC distribution network management topologies.

The short-sighted greedy method does not accommodate any long-term benefits with the real time optimization, so it is noted from Fig. 10 that batteries discharge during first 4 h (which are comparatively low energy price periods) and have lost all its initial stored energy. Therefore, during mid-peak (5th and 6th hours) and peak (hour 10–12) price hours, battery cannot support to meet the load demand. Hence the overall energy cost and network loss are highest among all the three methods (see Table 4). Further, due to non-consideration of VVC safety limits, the total tap operations of voltage regulator and switching of C2 are beyond the maximum allowable limits. Constraint (91) in the greedy imposes restriction on the load curtailment operation at every time step. Therefore, the time average load curtailment values at both AC and DC buses are very low (Fig. 11). As a result of described battery and low load curtailment operations, the cumulative energy cost at every time step is highest for the greedy process (Fig. 12).

Unlike real time greedy method, for the proposed method the battery charging and discharging operations try to follow the energy price variation, therefore charging occurs at low energy price hours and discharging occurs at mid-peak and peak energy price hours (see Fig. 10). Similar to the offline method, the total number of operations of VVC devices are also below their corresponding maximum allowable boundary values (see Table 4). Again, with rolling time the time average load curtailment values for both AC and DC buses go down the service limit (Fig. 11). As, the load curtailment is regulated considering the long-term aspects, so the cumulative energy cost at every time step is lower compared to the greedy method and the values are close to the offline curve (Fig. 12). The total energy cost and network loss values are also lesser compared to the existing real time greedy methods. Therefore, it is worthy to conclude that the proposed real time AC-DC distribution network management process can successfully consider the long-term offline benefits with the real time input data.

5.6. *Convergence Comparison between proposed iterative MILP and other existing solution methods*

The proposed iterative MILP method adopts certain linearization methods to simplify the non-linear expressions in the original MINCP framework. First order Taylor series and tangential cutting planes are used to approximate the quadratic expressions in (12), (25), (26), (30), (34) and (36) as their linear counterparts. Generally, these linearization methods deviate the solution point from the actual global optimal points. Therefore, to check the convergence and solution quality of the proposed iterative MILP method, further investigations are carried out by comparing the simulation results with three existing solution algorithms used in the literatures viz. mixed integer convex programming by adopting convex relaxations [39], MILP by performing piecewise linearization [8,28], and successive MILP (s-MILP) [45]. The simulation outcomes and the convergence curves are provided in Table 5 and Fig. 13, respectively. It is noted from the convergence curves for the iterative algorithms that initially the mismatch between objective function values for two consecutive iterations are large but with rolling iterations they converge and the mismatch values fall below the tolerance limit.

SOCP or convex relaxations are adopted for quadratic equality constraints (25), (30) and (34) to convert the original MINCP problem into a MICP by considering the equalities as inequalities. Gao et al. [39] have proved that the convex relaxation of the original problem can provide near global optimal solution for the AC-DC distribution network energy management. In this study, the relaxed MICP is solved by outer approximation (OA) algorithm as OA outperforms other decomposition methods (like Benders' decomposition) to solve mixed integer convex problems [51]. As OA solves a convex problem and a MILP problem at every iteration, so the iteration time is comparatively high (average 1.23 min per iteration). To solve the proposed real time, OA terminates after completing 15 iterations (average). The convergence curve at maximum loading hour is shown in Fig. 13. Further, the initialization before starting iteration is done by integer relaxed convex problem, which takes almost 2.3 min to determine the initial point. Therefore, the total solution time is almost 20.75 min at every time step, which is quite high for real time algorithms. However, as it guarantees global optimality, so certainly the solutions (i.e., total energy cost and network loss values given in Table 5) obtained by OA can serve as the reference for

other solution algorithms.

Piecewise linearization is a process to represent the quadratic terms in the constraints (12), (25), (26), (30), (34) and (36) as a sum of multiple linear segments [8,28]. This method is simple and does not need any iterative process. However, the performance of such linearization process highly depends upon the number of linear segments. Therefore, in this study total number of segments are varied from 2 to 20 and the simulation results are summarized in Table 5. Comparing with the base case (i.e., solution of OA), the error level reduces with increasing number of segments. However, higher level of accuracy is obtained in expense of more solution time because a greater number of segments add extra linear constraints and decision variables into the optimization problem. Further, the error level becomes nearly stable if the number of segments crosses 15 but the solution time increases significantly.

Previously author also proposed a successive MILP (s-MILP) algorithm in [45] to solve the day ahead energy management problem of AC-DC distribution network. The method determines the initial point by solving an integer relaxed non-convex problem (which takes almost 3.4 min to determine the initial point) and solves a MILP at each iteration (only Taylor series are considered to approximate the quadratic terms). The s-MILP algorithm requires approximately 7 iterations to converge at the solution point with 0.3446 % of error level (see Table 5). Each iteration takes 50 s times. The convergence curve of s-MILP at maximum loading hour is shown in Fig. 13. Therefore, the total solution time is approximately 9.3 min at every time step.

Comparing with the previously described three solution methods in Table 5 and Fig. 13, it is noted that the proposed iterative MILP algorithm outperforms them as far as the solution quality and convergence time at each time step are concerned. Unlike OA and s-MILP, the proposed algorithm does not need any rigorous nonlinear solution method to determine the initial point. However, with the median initial point the algorithm can converge by completing only 4 iterations and each iteration takes only 55 s. This happened as the infeasible solutions are taken care of by adding linear tangential cutting plane constraints. Therefore, the solution time is only 3.67 min. The convergence curve of iterative MILP at maximum loading hour is shown in Fig. 13. Further the error level is only 0.1377 %. Though the convergence time is more compared to the piecewise method with 2, 5 and 10 segments, but the error level is significantly lesser compared to them. Again, though the error levels for piecewise method with 15 and 20 segments are lower compared to the proposed iterative MILP but their solution time is quite high. Hence, it is pertinent to conclude that the proposed iterative MILP algorithm can determine the optimal decisions for the real time AC-DC distribution network energy management problem in less time and computation effort (as here only linear constraints are solved).

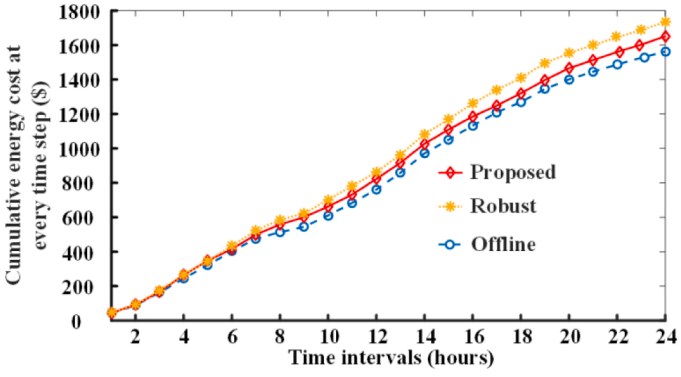

Fig. 14. Comparison between proposed and robust optimization (solved by HS algorithm) methods in terms of cumulative energy cost at every time step ($).

Table 6
Comparison of simulation outcomes between proposed and offline robust optimization (solved by HS algorithm) methods.

Evaluated parameter	Methods	
	Offline robust	Proposed
Optimal peak load (kW)	4178.14	3945.68
Optimal total network loss (MW)	1.9175	1.8868
Total energy cost ($)	1734.72	1650.46
Total tap operations by voltage regulator	58	51
Total C1 switching	5	5
Total C2 switching	6	5

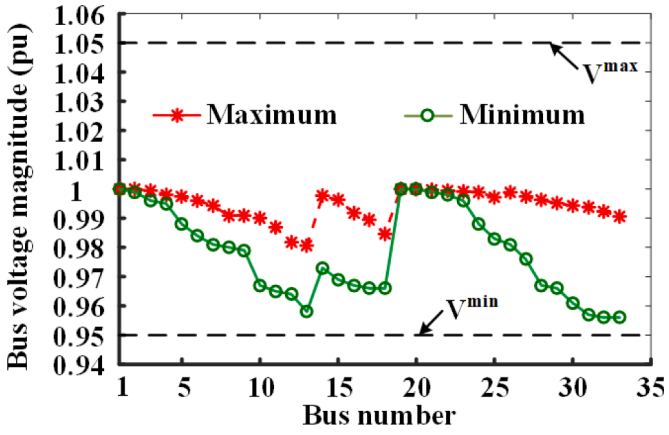

Fig. 15. Maximum and minimum voltage magnitude plot.

5.7. Comparison between the proposed real time and offline robust optimization frameworks

In section 5.5, the proposed real time algorithm is compared with the deterministic offline optimization problem. However, for assessing the worst case real time possibility, robust optimization frameworks are developed [63,64]. In this section, first a brief modelling of the robust optimization problem for the concerned AC-DC network energy management is described followed by the comparative analyses. Here, authors have adopted the robust optimization model proposed in [64].

In case of robust optimization, the uncertainty in the input data is generally realized by uncertainty sets to include all possible values of the uncertain parameters. In the proposed optimization problem, uncertainty can be experienced for load demand, solar power generation and energy price. However, in this case we are restricting our study only for load and solar power generation uncertainties. Let, $X_{i,t}$ denotes the uncertain parameter value at a bus 'i' at time period 't'. Hence, $X_{i,t}$ will consist of a forecasted value ($X^f_{i,t}$) plus an error component ($\zeta_{i,t}a_{i,t}$) [64] as written below.

$$X_{i,t} = X^f_{i,t} + \zeta_{i,t}a_{i,t} \tag{92}$$

here, $a_{i,t} \in \{0,1\}$ is a binary variable used to signify the bus which is experiencing the uncertainties. $\zeta_{i,t}$ is the level of the uncertainty and it is considered to be some fraction of the forecasted data. Therefore, the uncertainty set for the entire day is given by [64],

$$\mathbb{N}^t = \left\{ \begin{array}{c} X_{i,t}, \forall i \in [N_{ac}, N_{dc}] \,|X_{i,t} = X^f_{i,t} + \zeta_{i,t}a_{i,t}, \zeta_{i,t} \in \left[-\widehat{\zeta}_{i,t}, +\widehat{\zeta}_{i,t}\right], \\ a_{i,t} \in \{0,1\}, \forall i \in [N_{ac}, N_{dc}], \sum\limits_{i\in[N_{ac},N_{dc}]} a_{i,t} \leqslant \Upsilon^t \end{array} \right\} \tag{93}$$

here, Υ^t controls the number of buses where the load and solar generation uncertainties are present. For, $\Upsilon^t = 0$ there is no uncertainty i.e., the optimization problem is same as the offline deterministic problem described in section 4.1. Again, the worst-case possibility i.e., most

conservative solution will be attained when $\Upsilon^t = N_{ac} + N_{dc}$ i.e., 33 in this case. Therefore, the robust counterpart of the proposed AC-DC distribution network problem is as follows,

$$\left.\begin{array}{l} \min\left(\max_{X\in\mathbb{N}} \sum_{t\in T} C_t\right) \\ \text{subject to, (1) - (4), (6) - (17), and (20) - (39)} \end{array}\right\} \quad (94)$$

Now, same as [64], in this article the min–max problem of the robust optimization is solved by using Harmony Search (HS) algorithm. It is also proved in [64] that HS algorithm is better than other optimization techniques to solve such problems. The outcomes are shown in Fig. 14 and Table 6 for $\Upsilon^t = 33$ and $\widehat{\zeta}_{i,t} = 0.1 \times X^f_{i,t}$(i.e., 10 % error is considered on the forecasted data).

It is noted from Fig. 14 that as robust optimization seeks for worst possible objective function values for all possible uncertain conditions, so the cumulative energy cost deviated significantly from the deterministic offline case and the worst case values are even more than the real time results. Again, Table 6 shows that though the robust optimization follows the VVC device constraints and keep their operations below the safe limits but they are close to their corresponding boundary limits. Further, peak load and total loss values are also more than the proposed real time method. This implies that to anticipate the future real time condition, the robust method is deviating the optimal decisions much from the exact solution (i.e. the deterministic one). However, the proposed real time algorithm takes the real time online data and its optimal decisions are much closer to the deterministic solutions, which shows the superiority of the proposed method over the offline robust optimization algorithms.

5.8. Feasibility analysis of the derived optimal decisions

In this section, feasibility of the obtained optimal decisions is analysed. The optimal decisions are said to be OPF feasible if they follow the system security and reliability concerns. Now, in the formulation voltage limits are considered as network security concerns and different long term advantages (like frequent operations of the VVC devices and multiple load shedding) are accounted as the reliability concerns.

The maximum and minimum pu voltage magnitude experienced by each bus due to the varying load profile are noted and shown in Fig. 15. It is noted that the chance of overvoltage is low as here we are performing load shedding because of network stress. However, the proposed method can successfully overcome the chance of under voltage issue by keeping the minimum bus voltage above the minimum boundary limit (i.e. 0.95 pu). This shows that the proposed algorithm strictly obeys the network security constraint and eliminate the chance of voltage instability due to the implementation of the obtained optimal decisions.

It is already evident from Table 2, Fig. 7 and Fig. 8 that the proposed algorithm determines the optimal decisions by following the reliability concerns as well. That is why the total voltage regulator tap operations and capacitor bank switching are below their corresponding safety limits. Further, the load shedding operation is also distributed and in long run it is kept below the service quality limit for every bus. Hence, it is pertinent to conclude that the obtained optimal decisions strictly follow the system security and reliability concerns and also provide the most energy efficient operation to the AC-DC distribution network.

6. Conclusions

Penetration of direct current distributed energy resources motivates the power sector to build AC-DC distribution networks to minimize the power conversion losses. In need of developing efficient energy management portfolio of AC-DC distribution network, this article elucidates a novel MINCP based real time optimization framework by merging load curtailment and CVR. The proposed MINCP considers offline long-term benefits as time coupled stochastic expressions in the real time energy management problem. Later the MINCP framework is simplified by adopting certain linearization techniques, virtual queues and Lyapunov functions. The simplified MILP is initialized by the median values of the decision variables and solved iteratively to obtain the global optimal of the original MINCP. Further, to avoid infeasibilities, tangential cutting plane constraints are derived and added with the MILP formulation to bring back the solutions into feasible region in the following iterations. Stringent simulation is performed on 33-bus AC-DC network and looking at the outcomes the below mentioned conclusions are made:

1. Merger of real time load curtailment and CVR reduces the peak load and total network loss by 19.2277 % and 13.2586 %, respectively, and also keeps the VVC device operations within their corresponding safety limits. The network loss reduction depicts energy efficient operation of the network.
2. The proposed method deployed load curtailment operation in distributed manner that a certain bus must not experience frequent load shedding. This certainly keeps the service quality below the dissatisfaction limit.
3. The proposed iterative MILP solution process produces feasible optimal decisions with less computation effort and time (approximately 3.67 min) compared to the existing state of the art methods.

In this study, the AC network side of the AC-DC distribution system is modelled as a balanced three phase system. However, the same study can also be extended for unbalanced AC network by modelling the AC network resources, i.e., load, VVC devices and distributed energy resources, in per phase basis (as the unbalancing effect will only be seen in the DC side) as suggested in [65]. Further, the power flow equations of the AC network i.e., constraints (20) -(26), must also be modelled in per phase basis by either following the nonlinear branch flow model of [65] considering mutual coupling among the phases, or the linear branch flow model of [66] by neglecting the phase coupling. The DC network and VSC models will remain same as shown in this article. Therefore, only by revising the mathematical expressions of AC side resources and hence the simplifications corresponding to them in per phase basis by following the discussed methods, the proposed technique can be implemented directly on an unbalanced AC-DC distribution network with single phase loads and generations.

CRediT authorship contribution statement

Subho Paul: Conceptualization, Methodology, Software, Validation, Investigation, Writing – original draft, Writing – review & editing. **Narayana Prasad Padhy:** Supervision, Writing – review & editing.

Declaration of Competing Interest

The authors declare that they have no known competing financial interests or personal relationships that could have appeared to influence the work reported in this paper.

Data availability

Data will be made available on request.

Appendix A. Proof of Lemma 1

Definition of Lyapunov function in (66) says,

$$[L(\mathbb{N}_{t+1}) - L(\mathbb{N}_t)] = \frac{1}{2}\sum_{i\in[N_{AC},N_{DC}]}\left[\begin{array}{c}\rho\left(\left(\mathbb{R}^l_{i,t+1}\right)^2 - \left(\mathbb{R}^l_{i,t}\right)^2\right) + \sigma\left(\left(\mathbb{R}^l_{i,t+1}\right)^2 - \left(\mathbb{R}^{vr}_{i,t}\right)^2\right)\\ +\varepsilon\left(\left(\mathbb{R}^{cb}_{i,t+1}\right)^2 - \left(\mathbb{R}^{cb}_{i,t}\right)^2\right) + \varphi\left(\left(\mathbb{R}^b_{i,t+1}\right)^2 - \left(\mathbb{R}^b_{i,t}\right)^2\right)\end{array}\right] \tag{a1}$$

Now, from lemma 1 in [58] and load curtailment queue definition (61),

$$\left(\mathbb{R}^l_{i,t+1}\right)^2 - \left(\mathbb{R}^l_{i,t}\right)^2 \leqslant 2\mathbb{R}^l_{i,t}\left[\frac{p^{l,max}_{i,t} - p^l_{i,t}}{p^{l,max}_{i,t} - p^{l,\min}_{i,t}} - \beta_i\right] + \left(1 + (\beta_i)^2\right) \tag{a2}$$

As can be noted from tap changing and capacitor bank switching queue definitions in (62) and (63), that these two queues are looking similar to load curtailment queue (61). Hence, like (a2) the maximum value inequality can also be written for these two queues.

$$\left(\mathbb{R}^l_{i,t+1}\right)^2 - \left(\mathbb{R}^{vr}_{i,t}\right)^2 \leqslant 2\mathbb{R}^{vr}_{i,t}\left[h^{vr}_{i,t} - \xi^{vr}_i\right] + \left(1 + \left(\xi^{vr}_i\right)^2\right) \tag{a3}$$

$$\left(\mathbb{R}^{cb}_{i,t+1}\right)^2 - \left(\mathbb{R}^{cb}_{i,t}\right)^2 \leqslant 2\mathbb{R}^{cb}_{i,t}\left[a^{cb}_{i,t} - \xi^{cb}_i\right] + \left(1 + \left(\xi^{cb}_i\right)^2\right) \tag{a4}$$

Further, battery queue definition (64) says

$$\left(\mathbb{R}^b_{i,t+1}\right)^2 - \left(\mathbb{R}^b_{i,t}\right)^2 = 2\mathbb{R}^b_{i,t}\left(p^b_{i,t}\Delta t\right) + \left(p^b_{i,t}\Delta t\right)^2 \tag{a5}$$

Now, this can be upper bounded by

$$\left(\mathbb{R}^b_{i,t+1}\right)^2 - \left(\mathbb{R}^b_{i,t}\right)^2 \leqslant 2\mathbb{R}^b_{i,t}\left(p^b_{i,t}\Delta t\right) + \left(p^{b\max}_i \Delta t\right)^2 \tag{a6}$$

Substituting the boundary limits from (a2) -(a4) and (a6) into (a1), we get

$$[L(\mathbb{N}_{t+1}) - L(\mathbb{N}_t)] \leqslant 0.5\sum_{i\in[N_{AC},N_{DC}]}\left[\begin{array}{c}2\rho\mathbb{R}^l_{i,t}\left[\frac{p^{l,max}_{i,t} - p^l_{i,t}}{p^{l,max}_{i,t} - p^{l,\min}_{i,t}} - \beta_i\right] + \rho\left(1 + (\beta_i)^2\right) + 2\sigma\mathbb{R}^{vr}_{i,t}\left[h^{vr}_{i,t} - \xi^{vr}_i\right] + \sigma\left(1 + \left(\xi^{vr}_i\right)^2\right)\\ +2\varepsilon\mathbb{R}^{cb}_{i,t}\left[a^{cb}_{i,t} - \xi^{cb}_i\right] + \varepsilon\left(1 + \left(\xi^{cb}_i\right)^2\right) + 2\varphi\mathbb{R}^b_{i,t}\left(p^b_{i,t}\Delta t\right) + \varphi\left(p^{b\max}_i \Delta t\right)^2\end{array}\right]$$

$$\Rightarrow [L(\mathbb{N}_{t+1}) - L(\mathbb{N}_t)] \leqslant 0.5\sum_{i\in[N_{AC},N_{DC}]}\left[\begin{array}{c}\rho\left(1 + (\beta_i)^2\right) + \sigma\left(1 + \left(\xi^{vr}_i\right)^2\right)\\ +\varepsilon\left(1 + \left(\xi^{cb}_i\right)^2\right) + \varphi\left(p^{b\max}_i \Delta t\right)^2\end{array}\right] + \sum_{i\in[N_{AC},N_{DC}]}\left[\begin{array}{c}\rho\mathbb{R}^l_{i,t}\left[\frac{p^{l,max}_{i,t} - p^l_{i,t}}{p^{l,max}_{i,t} - p^{l,\min}_{i,t}} - \beta_i\right] + \varphi\mathbb{R}^b_{i,t}\left(p^b_{i,t}\Delta t\right)^2\\ +\sigma\mathbb{R}^{vr}_{i,t}\left[h^{vr}_{i,t} - \xi^{vr}_i\right] + \varepsilon\mathbb{R}^{cb}_{i,t}\left[a^{cb}_{i,t} - \xi^{cb}_i\right]\end{array}\right]$$

$$\Rightarrow [L(\mathbb{N}_{t+1}) - L(\mathbb{N}_t)] \leqslant O + \sum_{i\in[N_{AC},N_{DC}]}\left[\begin{array}{c}\rho\mathbb{R}^l_{i,t}\left[\frac{p^{l,max}_{i,t} - p^l_{i,t}}{p^{l,max}_{i,t} - p^{l,\min}_{i,t}} - \beta_i\right] + \sigma\mathbb{R}^{vr}_{i,t}\left[h^{vr}_{i,t} - \xi^{vr}_i\right] +\\ \varepsilon\mathbb{R}^{cb}_{i,t}\left[a^{cb}_{i,t} - \xi^{cb}_i\right] + \varphi\mathbb{R}^b_{i,t}\left(p^b_{i,t}\Delta t\right)^2\end{array}\right] \tag{a7}$$

$$O = 0.5\sum_{i\in[N_{AC},N_{DC}]}\left[\rho\left(1 + (\beta_i)^2\right) + \sigma\left(1 + \left(\xi^{vr}_i\right)^2\right) + \varepsilon\left(1 + \left(\xi^{cb}_i\right)^2\right) + \varphi\left(p^{b\max}_i \Delta t\right)^2\right]$$

Adding $W \times C_t$ at both sides of (a7),

$$[L(\mathbb{N}_{t+1}) - L(\mathbb{N}_t)] + W \times C_t \leqslant O + \sum_{i\in[N_{AC},N_{DC}]}\left[\begin{array}{c}\rho\mathbb{R}^l_{i,t}\left[\frac{p^{l,max}_{i,t} - p^l_{i,t}}{p^{l,max}_{i,t} - p^{l,\min}_{i,t}} - \beta_i\right] + \sigma\mathbb{R}^{vr}_{i,t}\left[h^{vr}_{i,t} - \xi^{vr}_i\right]\\ +\varepsilon\mathbb{R}^{cb}_{i,t}\left[a^{cb}_{i,t} - \xi^{cb}_i\right] + \varphi\mathbb{R}^b_{i,t}\left(p^b_{i,t}\Delta t\right)^2\end{array}\right] + W \times C_t \tag{a8}$$

Taking conditional expectation at both sides of (a8) with respect to $\mathbb{N}_t$, we get

$$\mathrm{E}[(L(\mathbb{N}_{t+1}) - L(\mathbb{N}_t))\,|\mathbb{N}_t] + W \times \mathrm{E}[C_t|\mathbb{N}_t]$$

$$\leqslant O + \sum_{i\in[N_{AC},N_{DC}]} \left(\begin{array}{c} \rho\mathbb{R}^{l}_{i,t}\mathrm{E}\left[\dfrac{p^{l,max}_{i,t} - p^{l}_{i,t}}{p^{l,max}_{i,t} - p^{l,\min}_{i,t}} - \beta_i \middle| \mathbb{N}_t\right] + \sigma\mathbb{R}^{vr}_{i,t}\mathrm{E}\left[h^{vr}_{i,t} - \xi^{vr}_{i} \middle| \mathbb{N}_t\right] \\ +\varepsilon\mathbb{R}^{cb}_{i,t}\mathrm{E}\left[a^{cb}_{i,t} - \xi^{cb}_{i} \middle| \mathbb{N}_t\right] + \varphi\mathbb{R}^{b}_{i,t}\mathrm{E}\left[p^{b}_{i,t}\Delta t \middle| \mathbb{N}_t\right] \end{array} \right) + W \times \mathrm{E}[C_t|\mathbb{N}_t]$$

$$\Rightarrow U_t \leqslant O + \sum_{i\in[N_{AC},N_{DC}]} \left(\begin{array}{c} \rho\mathbb{R}^{l}_{i,t}\mathrm{E}\left[\dfrac{p^{l,max}_{i,t} - p^{l}_{i,t}}{p^{l,max}_{i,t} - p^{l,\min}_{i,t}} - \beta_i \middle| \mathbb{N}_t\right] + \sigma\mathbb{R}^{vr}_{i,t}\mathrm{E}\left[h^{vr}_{i,t} - \xi^{vr}_{i} \middle| \mathbb{N}_t\right] \\ +\varepsilon\mathbb{R}^{cb}_{i,t}\mathrm{E}\left[a^{cb}_{i,t} - \xi^{cb}_{i} \middle| \mathbb{N}_t\right] + \varphi\mathbb{R}^{b}_{i,t}\mathrm{E}\left[p^{b}_{i,t}\Delta t \middle| \mathbb{N}_t\right] \end{array} \right) + W \times \mathrm{E}[C_t|\mathbb{N}_t] \text{(Proved)}$$

Appendix B. . Proof of Remark 1

The optimal decisions are obtained by solving optimization problem (70), which mainly aims to keep the values of the virtual queues at zero values. Therefore, we need to determine whether the AC-DC network is operating under stable condition for $\mathbb{R}^{l}_{i,f} = \mathbb{R}^{vr}_{i,f} = \mathbb{R}^{cb}_{i,f} = \mathbb{R}^{b}_{i,f} = 0$, where $\mathbb{R}_{i,f}$ denotes the values of the virtual queues at the optimal condition.

According to the Lyapunov stability criterion, the AC-DC network is asymptotically stable at the optimal decision point (where $\mathbb{R}^{l}_{i,f} = \mathbb{R}^{vr}_{i,f} = \mathbb{R}^{cb}_{i,f} = \mathbb{R}^{b}_{i,f} = 0$), if the Lyapunov function $L(\mathbb{N}_t)$, $\mathbb{N}_t = \left[\mathbb{R}^{l}_{i,t}, \mathbb{R}^{vr}_{i,t}, \mathbb{R}^{cb}_{i,t}, \mathbb{R}^{b}_{i,t}\right]$ satisfies the following conditions at the neighbourhood U of the optimal point [67].

1. $L(0) = 0$
2. $L(\mathbb{N}_t) > 0$ for all $\mathbb{N}_t \in U\backslash\{0\}$
3. $dL(\mathbb{N}_t)/dt \leqslant 0$ for all $\mathbb{N}_t \in U$

Now, the Lyapunov function defined in this article is as follows

$$L(\mathbb{N}_t) = \frac{1}{2}\sum_{i\in[N_{AC},N_{DC}]}\left[\rho\left(\mathbb{R}^{l}_{i,t}\right)^2 + \sigma\left(\mathbb{R}^{vr}_{i,t}\right)^2 + \varepsilon\left(\mathbb{R}^{cb}_{i,t}\right)^2 + \varphi\left(\mathbb{R}^{b}_{i,t}\right)^2\right]$$

The stability criterions are checked below,

1. Putting $\mathbb{R}^{l}_{i,t} = \mathbb{R}^{vr}_{i,t} = \mathbb{R}^{cb}_{i,t} = \mathbb{R}^{b}_{i,t} = 0$ at the expression of Lyapunov function, $L(\mathbb{N}_t) = L(0) = 0$
2. As, Lyapunov function is formulated with all squared terms of the queue lengths, so for any value of the queue other than zero, $L(\mathbb{N}_t)$ will always take a positive value. Hence, $L(\mathbb{N}_t) > 0$ for all $\mathbb{N}_t \in U\backslash\{0\}$
3. Now

$$\frac{dL(\mathbb{N}_t)}{dt} = \frac{\partial L(\mathbb{N}_t)}{\partial \mathbb{R}^{l}_{i,t}}\frac{d\mathbb{R}^{l}_{i,t}}{dt} + \frac{\partial L(\mathbb{N}_t)}{\partial \mathbb{R}^{vr}_{i,t}}\frac{d\mathbb{R}^{vr}_{i,t}}{dt} + \frac{\partial L(\mathbb{N}_t)}{\partial \mathbb{R}^{cb}_{i,t}}\frac{d\mathbb{R}^{cb}_{i,t}}{dt} + \frac{\partial L(\mathbb{N}_t)}{\partial \mathbb{R}^{b}_{i,t}}\frac{d\mathbb{R}^{b}_{i,t}}{dt} \tag{b1}$$

hence,

$$\frac{dL(\mathbb{N}_t)}{dt} = \sum_{i\in[N_{AC},N_{DC}]}\left[\rho\mathbb{R}^{l}_{i,t}\frac{d\mathbb{R}^{l}_{i,t}}{dt} + \sigma\mathbb{R}^{vr}_{i,t}\frac{d\mathbb{R}^{vr}_{i,t}}{dt} + \varepsilon\mathbb{R}^{cb}_{i,t}\frac{d\mathbb{R}^{cb}_{i,t}}{dt} + \varphi\mathbb{R}^{b}_{i,t}\frac{d\mathbb{R}^{b}_{i,t}}{dt}\right] \tag{b2}$$

It is already mentioned in Section 3.2.2 that the revised optimization problem aims to minimize the Lyapunov drift i.e. it always tries to minimize the queue length increment with time. Therefore, under the proposed optimization framework, queue length tends to decrease with time. Hence, $\frac{d\mathbb{R}^{l}_{i,t}}{dt} < 0, \frac{d\mathbb{R}^{vr}_{i,t}}{dt} < 0, \frac{d\mathbb{R}^{cb}_{i,t}}{dt} < 0$, and $\frac{d\mathbb{R}^{b}_{i,t}}{dt} < 0$.

Hence, from (b2) we can say $\frac{dL(\mathbb{N}_t)}{dt} < 0$ in the neighbourhood, which satisfies criteria 3.

Therefore, $L(\mathbb{N}_t)$ satisfies all the three conditions of Lyapunov stability criterion. So, it can be concluded from the above discussion that with the proposed Lyapunov function (66), the optimal decisions obtained by solving problem (70) will always keep the AC-DC distribution network under stable operating condition. ■.

References

[1] Reed GF, Grainger BM, Sparacino AR, Mao ZH. Ship to grid: Medium-voltage dc concepts in theory and practice. IEEE Power Energy Magazine 2012;10(6):70–9.

[2] "Data and statistics," International Energy Agency, [Online]. Available: https://www.iea.org/data-and-statistics?country=WORLD&fuel=Energypenalty%20-@M%20******%20consumption&indicator=CO2Industry.

[3] Cao J, Du W, Wang HF. An improved corrective security constrained OPF for meshed AC/DC grids with multi-terminal VSC-HVDC. IEEE Trans Power Syst 2016;31(1):485–95.

[4] Pizano-Martinez A, Fuerte-Esquivel CR, Ambriz-Pérez H, Acha E. Modeling of VSC-Based HVDC systems for a newton-raphson OPF algorithm. IEEE Trans Power Syst 2007;22(4):1794–803.

[5] Rabiee A, Soroudi A. Stochastic multiperiod OPF model of power systems with HVDC-connected intermittent wind power generation. IEEE Trans Power Delivery 2014;29(1):336–44.

[6] Venzke A, Chatzivasileiadis S. Convex relaxations of probabilistic AC optimal power flow for interconnected AC and HVDC grids. IEEE Trans Power Syst 2019;34(4):2706–18.

[7] Li Y, Li Y, Li G, Zhao D, Chen C. Two-stage multi-objective OPF for AC/DC grids with VSC-HVDC: incorporating decisions analysis into optimization process. Energy 2018;147:286–96.

[8] González-Cabrera N, Castro LM, Gutiérrez-Alcaraz G, Tovar-Hernandez JH. Alternative approach for efficient OPF calculations in hybrid AC/DC power grids

with VSC-HVDC systems based on shift factors. Int J Electr Power Energy Syst 2021;124:106395.
[9] Sarhan S, El-Sehiemy RA, Shaheen AM, Gafar M. TLBO merged with studying effect for economic environmental energy management in high voltage AC networks hybridized with multi-terminal DC lines. Appl Soft Comput 2023;143(110426):1–31.
[10] Paul S, Padhy NP. Resilient scheduling portfolio of residential devices and plug-in electric vehicle by minimizing conditional value at risk. IEEE Trans Ind Inf 2019;15(3):1566–78.
[11] Zhao C, Dong S, Li F, Song Y. Optimal home energy management system with mixed types of loads. CSEE J Power Energy Syst 2015;1(4):29–37.
[12] Kim HJ, Kim KM, Lee JW. A two-stage stochastic p-robust optimal energy trading management in microgrid operation considering uncertainty with hybrid demand response. Electrical Power and Energy Systems 2021;124(106422):1–16.
[13] Li Z, Xie X, Cheng Z, Zhi C, Si J. A novel two-stage energy management of hybrid AC/DC microgrid considering frequency security constraints. Int J Electr Power Energy Syst 2023;146(108768):1–12.
[14] Çimen H, et al. An online energy management system for AC/DC residential microgrids supported by non-intrusive load monitoring. Appl Energy 2022;307(118136):1–12.
[15] Kim TG, Lee H, An CG, Yi J, Won CY. Hybrid AC/DC microgrid energy management strategy based on two-step ANN. Energies 2013;16(4):1787.
[16] Thirugnanam K, El Moursi MS, Khadkikar V, Zeineldin HH, Al Hosani M. Energy management strategy of a reconfigurable grid-tied hybrid AC/DC microgrid for commercial building applications. IEEE Trans Smart Grid 2022;13(3):1720–38.
[17] Tylavsky DJ, Trutt FC. The Newton-Raphson load flow applied to AC/DC systems with commutation impedance. IEEE Trans Ind Appl 1983;19(6):940–8.
[18] Ahmed HMA, Eltantawy AB, Salama MMA. A generalized approach to the load flow analysis of AC-DC hybrid distribution systems. IEEE Trans Power Syst 2018;33(2):2117–27.
[19] Molaee ZS, Rokrok E, Doostizadeh M. A unified power flow approach using VSC-efficiency for AC-DC distribution systems operating at grid connected and islanded modes. Int J Electr Power Energy Syst 2021;130:106906.
[20] Murari K, Padhy NP, Kamalasadan S. "Backward-Forward Sweep Based Power Flow Algorithm for Radial and Meshed AC-DC Distribution System", in 2021 IEEE Industry Applications Society Annual Meeting (IAS). BC, Canada: Vancouver; 2021.
[21] Murari K, Padhy NP. Graph-theoretic-based approach for solving load flow problem of AC–DC radial distribution network with distributed generations. IET Gener Transm Distrib 2020;14(2):5327–46.
[22] Murari K, Padhy NP. A network-topology based approach for the load flow solution of AC-DC distribution system with distributed generations. IEEE Trans Ind Inf 2019;15(3):1508–20.
[23] Molaee ZS, Rokrok E, Doostizadeh M. An optimal planning model for AC-DC distribution systems considering the converter lifetime. Int J Electr Power Energy Syst 2022;138:107911.
[24] Ahmed HMA, Eltantawy AB, Salama MMA. A planning approach for the network configuration of AC-DC hybrid distribution systems. IEEE Trans Smart Grid 2018;9(3):2203–13.
[25] Ghadiri A, Haghifam MR, Larimi SMM. Comprehensive approach for hybrid AC/DC distribution network planning using genetic algorithm. IET Gener Transm Distrib 2017;11(16):3892–902.
[26] Gao S, Jia H, Marnay C. Techno-economic evaluation of mixed AC and DC power distribution network for integrating large-scale photovoltaic power generation. IEEE Access 2019;7:105019–29.
[27] Zhang L, Chen Y, Shen C, Tang W, Liang J, Xu B. Optimal configuration of hybrid AC/DC urban distribution networks for high penetration renewable energy. IET Gener Transm Distrib 2018;12(20):4499–506.
[28] Ahmed HMA, Salama MMA. Energy management of AC–DC hybrid distribution systems considering network reconfiguration. IEEE Trans Power Syst 2019;34(6):4583–94.
[29] Qiao F, Ma J. Voltage/Var control for hybrid distribution networks using decomposition-based multiobjective evolutionary algorithm. IEEE Access 2020;8:12015–25.
[30] Qiao F, Ma J. Coordinated voltage/var control in a hybrid AC/DC distribution network. IET Gener Transmiss Distrib 2020;14(11):2029–137.
[31] Luo L, He P, Gu W, Sheng W, Liu K, Bai M. Coordinated scheduling of generalized energy storage in multi-voltage level AC/DC hybrid distribution network. J Storage Mater 2023;57:106189.
[32] Yu K, Xue B, Gu F, Hua H, Yuan Y, Li Q. A novel PET model based volt/var control of AC–DC hybrid distribution network. Energy Rep 2022;8:2672–85.
[33] Khan MO, Wadood A, Abid MI, Khurshaid T, Rhee SB. Minimization of network power losses in the AC-DC hybrid distribution network through network reconfiguration using soft open point. Electronics 2021;10(1-13):326.
[34] Zhu Z, Liu D, Liao Q, Tang F, Zhang JJ, Jiang H. Optimal power scheduling for a medium voltage AC/DC hybrid distribution network. Sustainability 2018;10(1–22):318.
[35] Alshammari K, Alrajhi H, El-Shatshat R. Optimal power flow for hybrid AC/MTDC systems. Arab J Sci Eng 2022;47:2977–86.
[36] Luo L, He P, Gu W, Sheng W, Liu K, Bai M. Temporal-spatial scheduling of electric vehicles in AC/DC distribution networks. Energy 2022;255:124512.
[37] Eajal AA, Shaaban MF, Ponnambalam K, El-Saadany EF. Stochastic centralized dispatch scheme for AC/DC hybrid smart distribution systems. IEEE Trans Sustainable Energy 2016;7(3):1046–59.
[38] Fu Y, Zhang Z, Li Z, Mi Y. Energy management for hybrid AC/DC distribution system with microgrid clusters using non-cooperative game theory and robust optimization. IEEE Trans Smart Grid Mar. 2020;11(2):1510–25.
[39] Gao H, Wang J, Liu Y, Wang LLJ. An improved ADMM-based distributed optimal operation model of AC/DC hybrid distribution network considering wind power uncertainties. IEEE Syst J 2021;15(2):2201–11.
[40] Xu Q, Zhao T, Xu Y, Xu Z, Wang P, Blaabjerg F. A distributed and robust energy management system for networked hybrid AC/DC microgrids. IEEE Trans Smart Grid 2020;11(4):3496–508.
[41] Geng Q, Hu Y, He J, Zhou Y, Zhao W, Xu X, et al. Optimal operation of AC–DC distributionnetwork with multi park integrated energysubnetworks considering flexibility. IET Renew Power Gener 2020;14(6):1004–19.
[42] Zhao D, Wang H, Tao R. Multi-time scale dispatch approach for an AC/DC hybrid distribution system considering the response uncertainty of flexible loads. Electr Pow Syst Res 2021;199:107394.
[43] Sun F, Ma J, Yu M, Wei W. A robust optimal coordinated droop control method for multiple VSCs in AC–DC distribution network. IEEE Trans Power Syst 2019;34(6):5002–11.
[44] Dong J, Zhao J, Liu Z, Li Y, Yu Z, Liu J, et al. Risk assessment of AC/DC hybrid distribution network considering new energy and electric vehicle access. Front Energy Res 2022;10:816246.
[45] Paul S, Sharma A, Padhy NP. Risk constrained energy efficient optimal operation of a converter governed AC/DC hybrid distribution network with distributed energy resources and volt-VAR controlling devices. IEEE Trans Ind Appl 2021;57(4):4263–77.
[46] Gholami K, Azizivahed A, Arefi A. Risk-oriented energy management strategy for electric vehicle fleets in hybrid AC-DC microgrids. J Storage Mater 2022;50(104258):1–16.
[47] Wu T, Wang J, Lu X, Du Y. AC/DC hybrid distribution network reconfiguration with microgrid formation using multi-agent soft actor-critic. Appl Energy 2022;307:118189.
[48] Shaaban MF, Eajal AA, El-Saadany EF. Coordinated charging of plug-in hybrid electric vehicles in smart hybrid AC/DC distribution systems. Renew Energy 2015;82:92–9.
[49] Azzouz MA, Shaaban MF, El-Saadany EF. Real-time optimal voltage regulation for distribution networks incorporating high penetration of PEVs. IEEE Trans Power Syst 2015;30(6):3234–45.
[50] Su Y, Teh J, Liu W. Hierarchical and distributed energy management framework for AC/DC hybrid distribution systems with massive dispatchable resources. Electr Pow Syst Res 2023;225(109856):1–14.
[51] Han D, Jian J, Yang L. Outer approximation and outer-inner approximation approaches for unit-commitment problem. IEEE Trans Power Syst 2014;29(2):505–13.
[52] Hossan MS, Chowdhury B. Integrated CVR and demand response framework for advanced distribution magagement systems. IEEE Trans Sustainable Energy Jan. 2020;11(1):534–44.
[53] Satsangi S, Kumbhar GB. Effect of load models on scheduling of VVCdevices in a distribution network. IET Gener Transm Distrib 2018;12(17):3993–4001.
[54] Mohan N, Undeland TM, Robbins WP. Power Electronics, Hoboken, NJ. USA: Wiley; 2002.
[55] Zhang Q, Dehghanpour K, Wang Z. Distributed CVR in unbalanced distribution systems with PV penetration. IEEE Trans Smart Grid Sep. 2019;10(5):5308–19.
[56] McCormick GP. Computability of global solutions to factorable nonconvex programs: part-I—convex underestimating problems. Math Program 1976;10(1):147–75.
[57] Shukla SR, Paudyal S, Almassalkhi MR. Efficient distribution system optimal power flow with discrete control of load tap changers. IEEE Trans Power Syst 2019;34(4):2970–9.
[58] Sun S, Dong M, Liang B. "Joint supply, demand, and energy storage management towards microgrid cost minimization", in Proc. Venice, Italy: IEEE Int. Conf. Smart Grid Commun; 2014.
[59] Zhou P, Hu X, Zhu Z, Ma J. What is the most suitable Lyapunov function? Chaos Solitons Fractals 2021;150(111154):1–6.
[60] Cheng D, Guo L, Huang J. On quadratic Lyapunov functions. IEEE Trans Autom Control 2003;48(5):885–90.
[61] Commonwealth edision company real time hourly prices, 18 June 2018. [Online]. Available: https://hourlypricing.comed.com/live-prices. [Accessed 30 Aug. 2019].
[62] Diaz-Aguiló M, et al. Field-Validated load model for the analysis of CVR in distribution secondary networks: energy conservation. IEEE Trans Power Delivery Oct. 2013;28(4):2428–36.
[63] Xu T, Ren Y, Guo L, Wang X, Liang L, Wu Y. Multi-objective robust optimization of active distribution networks considering uncertainties of photovoltaic. Int J Electr Power Energy Syst 2021;133(107197):1–10.
[64] Jeddi B, Vahidinasab V, Ramezanpour P, Aghaei J, Shafie-khah M, Catalão JP. Robust optimization framework for dynamic distributed energy resources planning. Int J Electr Power Energy Syst 2019;110:419–33.
[65] Paul S, Prasad R, Padhy NP. "A Sequential MILP Strategy for Energy Efficient Management of Unbalance Distribution Network", in 2021 IEEE Power & Energy Society General Meeting (PESGM). Washington: DC, USA; 2021.
[66] Gan L, Low SH. Convex relaxations and linear approximation for optimal power flow in multiphase radial networks. in *2014 Power Systems Computation Conference*. 2014.
[67] Khalil HK. "Lyapunov stability", in control systems, robotics and automation. Encyclopedia of Life Support Systems (EOLSS) 2009.